Urol Res (2010) 38:357–376
DOI 10.1007/s00240-010-0300-7

ORIGINAL PAPER

Face-specific incorporation of osteopontin into urinary and inorganic calcium oxalate monohydrate and dihydrate crystals

Lauren A. Thurgood · Alison F. Cook · Esben S. Sørensen · Rosemary L. Ryall

Received: 27 January 2010 / Accepted: 1 July 2010 / Published online: 22 July 2010

Abstract Our aim was to examine the attachment to, and incorporation of intact, highly phosphorylated osteopontin (OPN) into inorganic (i) and urinary (u) calcium oxalate monohydrate (COM) and dihydrate (COD) crystals. uCOM and uCOD crystals were precipitated from ultrafiltered (UF) urine containing human milk OPN (mOPN) labelled with Alexa Fluor 647 fluorescent dye at concentrations of 0.1–5.0 mg/L. iCOM and iCOD crystals were generated in aqueous solutions at concentrations of 0.01–0.5 mg/L. Crystals were demineralised with EDTA and the resulting extracts analysed by sodium dodecyl sulphate polyacrylamide gel electrophoresis and western blotting, or examined by fluorescent confocal microscopy and field emission scanning electron microscopy before and after washing to remove proteins bound reversibly to the crystal surfaces. Binding of mOPN to pre-formed iCOM crystals was also studied in phosphate-buffered saline (PBS) and ultrafiltered (UF) urine. mOPN attached to the {100} faces and to the {010} sides of the {100}/{010} edges of iCOM crystals was removed by washing, indicating that it was not incorporated into the mineral bulk. In both PBS and urine, mOPN was attached to the {021} faces of pre-formed iCOM crystals as well as to the {100}/{010} edges, but was concentrated at the intersection points of the {100} and {121} faces at the crystal tips. Attachment in UF urine appeared to be greater than in PBS and stronger at higher calcium concentrations than lower calcium concentrations. In uCOM crystals, the distribution of fluorescence and patterns of erosion after washing suggested attachment of mOPN to the four end faces, followed by interment within the mineral phase. Fluorescence distributions of mOPN associated with both iCOD and uCOD crystals were consistent with uniform binding of the protein to all equivalent {101} faces and concentration along the intersections between them. Persistence of fluorescence after washing indicated that most mOPN was incarcerated within the mineral phase. We concluded that attachment of mOPN to calcium oxalate crystals is face-specific and depends upon the anatomical and genetic source of the protein and whether the crystals are (1) COM or COD; (2) pre-formed or precipitated from solution, and (3) precipitated from urine or aqueous solutions. Our findings emphasise the need for caution when drawing conclusions about possible roles of OPN or other proteins in urolithiasis from experimental data obtained under inorganic conditions.

Keywords Osteopontin · Calcium oxalate dihydrate · Calcium oxalate monohydrate · Protein binding · Urolithiasis · Fluorescence confocal microscopy

L. A. Thurgood (✉) · A. F. Cook · R. L. Ryall
Urology Unit, Department of Surgery,
Flinders Medical Centre, Flinders Clinical and Molecular Medicine, School of Medicine, Flinders University,
Bedford Park, SA 5042, Australia
e-mail: rose.ryall@flinders.edu.au

E. S. Sørensen
Protein Chemistry Laboratory,
Department of Molecular Biology,
Aarhus University, Aarhus, Denmark

Introduction

Healthy biomineralisation is controlled by acidic macromolecules [1], which direct the nucleation, growth and morphology of biominerals using a combination of molecular templating and preferential adsorption onto specific crystal faces [2, 3]. Like all biominerals, kidney stones are associated with proteins. Conventionally referred to as the

organic matrix, the protein phase of renal stones has been reported to contain 50% aspartate and glutamate residues, both of which are highly acidic. Calcium oxalate (CaOx) crystals, which comprise the major mineral constituent of most human kidney stones, contain urinary proteins adsorbed onto their surfaces and incorporated within their mineral bulk [4, 5]. CaOx exists in kidney stones and urine as two distinct polymorphs: CaOx monohydrate (COM) and dihydrate (COD) (Fig. 1), which are associated with different proteins. Not all urinary proteins are present in each crystal type [5]; nor does their relative representation reflect their proportional amounts in urine [6]. One urinary protein, osteopontin (OPN), is an abundant [7] component of kidney stone matrix [8, 9] that is widely acknowledged to be a likely determinant of stone formation [10, 11].

OPN is a unique and complex protein. Its acidic properties result from a high content of phosphoserine, aspartate, and glutamate residues, which constitute over half of its amino acids [12]. In fact, aspartate alone accounts for 48 of the 298 amino acids in OPN's backbone [13]. The protein has a total molecular weight of 42.9 kDa of which post-translational modifications, primarily phosphorylation and glycosylation account for approximately 9 kDa [14]. On Sodium dodecyl sulphate polyacrylamide gel electrophoresis (SDS-PAGE), OPN migrates according to a molecular mass of approximately 66 kDa, but reported Mr values have ranged from as low as ~20–25 kDa to as high as 80 kDa [12], which can most likely be explained by poor SDS-pairing caused by the protein's high acidity. The protein has a completely unstructured polypeptide spine, allowing it to be highly flexible in solution and therefore able to associate with numerous binding partners, such as other proteins and minerals [15]. In inorganic solutions, OPN has been reported to inhibit the nucleation, growth and aggregation of COM [11, 16, 17] and the growth of hydroxyapatite (HA) crystals [18, 19]. Phosphorylation of OPN is essential for its role in biomineralisation, since it affects the protein's conformation, catalytic activities and cell-binding properties [20], and consequently, its mineral-binding capacity [21, 22], which determines its ability to inhibit the crystallisation of HA [23] and COM [21, 22]. OPN's mineral-binding properties may also influence the internalisation and subsequent removal of COM crystals in vivo. In rats, OPN surrounds microcrystals comprising stones formed in response to a lithogenic diet [24]. The OPN coating appears to mediate attachment of the crystals to macrophages and multinucleated cells in the surrounding interstitium [25, 26], which engulf and destroy them [27].

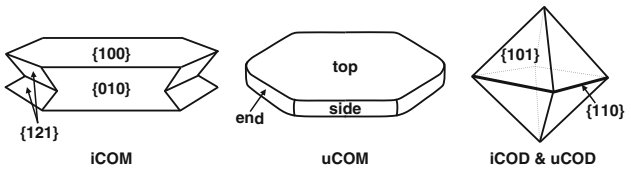

Fig. 1 Diagrammatic representation of inorganic (iCOM) and urinary (uCOM) calcium oxalate monohydrate and dihydrate (iCOD and uCOD) crystals generated in this study. The iCOD and uCOD crystal faces are numbered according to the system of Tazzoli and Domeneghetti [72], while the iCOM faces are labelled using the simplified notation used by Hunter and colleagues [21, 22, 39, 40, 68]. Although uCOM crystals have the same general hexagonal shape as the most common habit modification caused by additives [52], they exhibit significant rounding at the edges between faces comprising the crystal sides and ends, and classical Miller indices cannot be ascribed to them. Accordingly, the uCOM crystal faces are described simply as "*top*", "*side*" and "*end*"

Although COM is more commonly present in kidney stones [28], COD is more frequently excreted in urine [29, 30]. This difference suggests that structural features of COM crystals may increase their likelihood of being retained within the kidney, where they may act as nuclei for stone formation, while those of COD reduce the probability of their attachment to renal cells and consequent induction of calculogenesis. Thus, it has been proposed that preferential formation of COD, rather than COM crystals would protect against stone pathogenesis [31, 32]. OPN [33] and undifferentiated urinary proteins bound to the surfaces of COM crystals [34–36], and also incarcerated within them [36], inhibit the attachment of COM urinary crystals to renal epithelial cell membranes. It is possible therefore that the more frequent excretion of the dihydrate might result from differences between individual proteins associated with COM and COD crystals.

With one exception [37], investigations of physical interactions between OPN and CaOx crystals have focused on the monohydrate and have been performed under inorganic conditions. These facts are important, because they overlook the involvement of COD in stone disease, and because the association of OPN with COM crystals is affected by the medium in which binding is performed: OPN binds to COM under inorganic conditions [21, 22, 38], but is undetectable by western blotting in demineralised extracts of COM crystals precipitated from human urine [5]. Some investigators have also used synthetic OPN phosphopeptides rather than the intact protein molecule itself, in order to identify specific amino acid sequences involved in the protein's attachment to pre-formed COM crystals [39, 40], their effects on the morphology of COM crystals precipitated in their presence [39, 41] or their influence on COM crystal growth [40]. Although atomic force microscopy [38] and fluorescence confocal microscopy [21, 22] have been used to test the effects of intact OPN on COM crystal binding, morphology and growth, there are no published reports of the intracrystalline organisation of intact OPN within CaOx crystals precipitated from human urine containing the protein, or its distribution

upon the surfaces of pre-formed urinary COM or COD crystals.

Published findings suggest that OPN is likely to be involved in regulating the formation of CaOx crystals, their binding to renal epithelial cells, and their eventual removal, and may therefore play a directive role in urolithiasis. The aims of this study were (1) to examine, using confocal fluorescence microscopy and field emission scanning electron microscopy (FESEM), the face-specific attachment of OPN to pre-formed urinary and inorganic COM and COD crystals and (2) to determine the intracrystalline distribution of intact, highly phosphorylated OPN into COM and COD crystals precipitated from inorganic solutions and urine in the presence of the protein.

Materials and methods

All materials used were of analytical grade, unless otherwise mentioned. All solutions were prepared with high quality water from a "Hi Pure" water purification system (Permutit Australia, Brookvale, NSW, Australia).

Purification of human milk OPN (mOPN)

mOPN was purified from human milk from a pool of donors essentially as described previously [42]. However, instead of undergoing the final RP-HPLC step, the supernatant resulting from the barium chloride and sodium citrate precipitation was dialysed against 0.1% formic acid overnight and centrifuged (16,000 rpm, 25 min), and the resulting supernatant was lyophilised. N-terminal sequencing verified very high purity (+98%) of the resulting OPN. The phosphorylation status of this particular OPN preparation was analysed as described [14] and shown to contain an average of 32 phosphorylated residues.

Sodium dodecyl sulphate polyacrylamide gel electrophoresis

To demonstrate the purity of the mOPN, the lyophilised sample was mixed with reducing buffer stock, electrophoresed and stained with silver as described previously [35].

Western blotting

After electrophoresis, the proteins were transferred to a nitrocellulose membrane at 100 V for 1 h using pre-stained Mr standards (Seeblue, Novex Experimental Technologies, San Diego, CA, USA). Blots were blocked in 3% skim milk/PBS (blotto) for 1 h, washed three times with blotto containing 0.05% tween-20 for 5 min and immunoblotted using a polyclonal rabbit anti-human OPN antibody (Ab8448, Abcam, Cambridge, MA, USA) at a dilution of 1:1,000. Membranes were then washed as before and incubated for 1 h with a goat anti-rabbit IgG HRP conjugate (#1706515, Bio-Rad Laboratories Inc, Hercules, CA, USA) at a dilution of 1:2,000. The membrane was washed and developed using 0.06% (w/v) diaminobenzidine (DAB), to which hydrogen peroxide (0.1% v/v) had been added immediately before use.

Fluorescence labelling of mOPN

Purified mOPN was labelled using an Alexa Fluor 647 protein labelling kit (A3009, Molecular Probes, Inc., OR, USA) according to the manufacturer's recommendations. Briefly, this involved the addition of 2.3 µl of Alexa Fluor 647 to 100 µl of mOPN in a solution of phosphate-buffered saline (PBS 8.06 mM Na_2PO_4, 138 mM NaCl, and 2.67 mM KCl, 1.47 mM KH_2PO_4 pH 7.4) at a concentration of 1 mg/mL, and adjustment of the pH to 8.3 by the addition of 20 µL of 1 M disodium carbonate. The reaction was allowed to proceed for 15 min, after which the unconjugated dye was removed from the protein with the spin column and desalting resin provided in the kit. To determine the degree of labelling, the sample was read at an absorbance of 650 and 280 nm in a quartz cuvette.

Preparation of urine

This study was approved by the Flinders Clinical Research Ethics Committee. Fresh healthy human urine was collected from healthy volunteers (2 women, 2 men) with no history of stone disease, and the absence of nitrites and haematuria confirmed by dipstick (Combur7®, Roche Diagnostics, Germany). The urine was centrifuged (10,000 rpm, 20 min) at 4°C and pre-filtered (RW0314250: Millipore Corporation, Bedford, MA, USA), followed by filtration (0.22 µm: GVWP14250; Millipore Corporation) and ultrafiltration through a Millipore Prep/Scale Spiral Wound TFF-1 Module with a nominal Mr cut-off of 10 kDa (Millipore Corporation).

Preparation of urinary crystals in the presence of mOPN

The urine calcium concentration was measured by the *o*-cresophthalein complexone technique using a Hitachi 917 automated biochemical analyser at a wavelength of 546 nm. The calcium concentration was then adjusted, by the dropwise addition of 1 M $CaCl_2$ solution, to 2 mM for precipitation of urinary COM (uCOM) crystals, and to 8 mM for generation of urinary COD (uCOD) crystals. To determine the metastable limit (MSL), which is defined as the minimal amount of oxalate needed to produce detectable CaOx crystals, small aliquots of urine were titrated

with aqueous sodium oxalate (NaOx) solution [5]. Alexa Fluor-labelled mOPN was added to 15 mL aliquots of UF urine to give final concentrations of 0.1, 0.5, 1.0 and 5.0 mg/L. A load of NaOx solution, two steps above the MSL, was added and the samples were incubated in a shaking water bath (100 opm) at 37°C for 2 h. The precipitated crystals were removed from the urine by filtration (0.22 μm, Millipore) and washed copiously with distilled water to remove superficially bound OPN [43].

It has been reported previously that urinary OPN (uOPN) is not incorporated into COM crystals precipitated from human urine [5]. However, fluorescence was observed in COM crystals generated from UF urine containing mOPN at concentrations of 1 and 5 mg/L, even after washing with water. Crystals were therefore also washed with 0.1 M NaOH to ensure the complete removal of any remnant, loosely bound superficial protein [6, 43].

The concentration of uOPN in normal urine has been reported by various authors to span the range 0.01–5.8 mg/L [44–47]. In this study, urinary crystals were therefore precipitated at mOPN concentrations between 0 and 5 mg/L.

Preparation of inorganic COM (iCOM) and COD (iCOD) crystals

iCOM crystals were grown by the method of Cook et al. [48]. Using a syringe pump (Razel, model A-99), 7.5 mL of 5 mM $CaCl_2$ solution containing different concentrations of Alexa Fluor-labelled mOPN was added slowly to 7.5 mL of 5 mM NaOx solution in a shaking water bath (100 opm) over a 2.5-h period and the flasks were then refrigerated at 4°C for ~48 h. Additives affect CaOx crystallisation in inorganic solutions at concentrations approximately 1/10th–1/100th of those required in undiluted urine [49]. The final OPN concentrations used to prepare inorganic crystals were therefore 0, 0.01, 0.05, 0.1 and 0.5 mg/L.

Additional iCOM crystals prepared using the same method, but with no added mOPN, were generated, washed thoroughly with water, lyophilised, and stored at −80°C for later use. They were then incubated (1 mg/mL) in PBS or in UF urine containing OPN at a concentration of 1 mg/L for 2 h at calcium concentrations of 2 and 8 mM. Inorganic COD crystals (iCOD) were generated using the method of Brown et al. [50] which entailed the addition of 500 mL 25.1 mM $CaCl_2$ and 500 mL 6.4 mM NaOx dropwise to a solution containing 38.5 mM tri-sodium citrate, 46.2 mM $MgSO_4$ and 254.8 mM of KCl. Crystals were harvested via filtration (0.22 μm, Millipore), washed gently with distilled water and lyophilised.

Controls consisted of crystals generated in the absence of mOPN. Additional controls comprised crystals grown without protein in the presence of Alexa Fluor 647 at dye concentrations equivalent to the amount of dye calculated to bind at the highest OPN concentration. All control crystals were washed copiously with water or NaOH to match their experimental counterparts.

Demineralisation of crystals and analysis by SDS-PAGE and western blotting

Crystals were demineralised in 0.25 M EDTA (pH 8.0) at a ratio of 12 mg/mL overnight at 4°C. The resulting solution was electrodialysed against a tris/glycine buffer (25 mM Tris, 0.2 M glycine, pH 8.3) at 40 V at 4 h, followed by a 50% buffer solution for 4 h at 60 V. The buffer was replaced with distilled water and the sample was electrodialysed at 100 V, with six water changes over a 48-h period. The resulting extracts were lyophilised and mixed with reducing sample buffer, electrophoresed on a 9–18% gradient gel, and silver stained as described previously [43]. For western blotting, the samples were electrophoretically transferred to a nitrocellulose membrane and immunoblotted using a polyclonal OPN antibody (Ab8448, Abcam, Cambridge, UK), as previously described [43].

Preparation of COM crystals with atypical morphologies

Additional COM crystals were prepared according to methods described in detail by Jung et al. [51], to produce three types of COM crystals with {010}, $\{1\bar{2}1\}$ or {100} faces oriented horizontally to the observer, to facilitate direct observation of OPN binding using confocal microscopy. The crystals (4 mg/mL) were incubated in PBS containing mOPN at a final concentration of 0.5 mg/L for 2 h in a shaking water bath at 37°C, removed by filtration, washed gently with distilled water and dried.

Examination of crystals by confocal microscopy

A Leica TCS SP5 scanning confocal microscope fitted with a 63× oil immersion objective (numerical aperture 1.4) was used to image mOPN inside the crystals. All procedures were carried out in the dark to prevent bleaching of the fluorochrome and to minimise the effects of scattered light. For transmission microscopy, the crystals were scanned with an Argon laser (488 nm) and imaged with a transmitted light detector. To excite the fluorochrome, crystals were scanned with a helium/neon laser (633 nm), and emission from 645 to 730 nm was imaged with a photomultiplier tube (PMT) detector with the pinhole set to 1 Airy unit. The PMT gain and offset remained the same throughout all experiments to allow continuity and direct comparison of the fluorescent intensity of different crystals.

Examination of crystals by FESEM

Crystal suspensions were filtered onto Nucleopore filters (0.22 μm, SPI supplies, West Chester, PA, USA). The filtration membranes were dried overnight at 37°C, mounted on aluminium stubs and coated with carbon to 3-nm thickness using a high vacuum evaporator (DV-502, Denton Vacuum Inc., Moorestown, NJ, USA). The stubs were examined using a Philips XL30 FEGSEM field emission scanning electron microscope at 10 kV accelerating voltage and 10 mm working distance.

Results

Protein analysis

The SDS-PAGE gel and western blot of the purified mOPN are shown in Fig. 2a. The protein appears predominantly as a single band migrating with an Mr of ~66 kDa, with some faint smearing between 35 and 40 kDa and the top of the gel. Western blotting (Fig. 2b) shows a single band at 66 kDa and smearing over the same Mr range as is seen in the gel.

Figure 3 depicts SDS-PAGE gels of urinary proteins and demineralised extracts of COM crystals used in this study, together with their corresponding western blots stained for OPN. Gels and blots of COD crystals were not performed, as we have already reported the incorporation of OPN into COD crystals [5]. Lane 2 shows proteins in centrifuged and filtered urine. As is always observed [5, 43], many protein bands are evident and it is not possible to discern distinct bands that can be ascribed specifically to OPN. In contrast, the accompanying blot shows OPN visible as a smear running between ~55 and ~90 kDa, which is typical of the pattern of uOPN [5]. In lane 3 are shown the proteins detected in COM crystals precipitated from the centrifuged and filtered urine. The associated western blot shows no evidence of uOPN, confirming, as has been reported previously [5] that uOPN is not incorporated to a significant degree into COM crystals precipitated from urine. As expected, lane 4 demonstrates the absence of any proteins >10 kDa from crystals deposited from the ultrafiltered urine sample. After addition of purified mOPN to the ultrafiltered urine the resulting demineralised matrix (lane 5) shows the presence of a single band migrating at ~64 kDa, which is comparable to that shown in the gel presented in Fig. 2, as well as a number of faintly staining bands extending from below 30 kDa to the top of the lane. The corresponding western blot contains a widely dispersed band extending above 64 kDa, as well as extensive smearing running from just above 30 kDa to the top of the lane, suggesting that incorporation of the mOPN into the crystal structure causes some molecular disruption and/or polymerisation of the protein and the resulting fragments, or perhaps the occurrence of some non-specific staining.

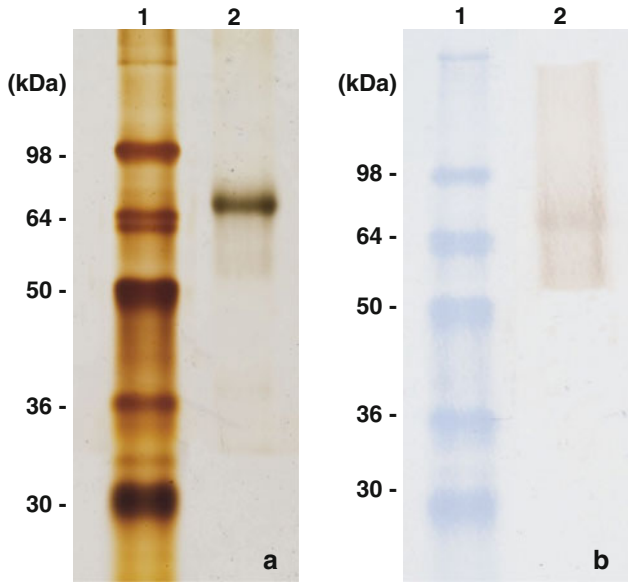

Fig. 2 SDS-PAGE (**a**) and western blot (**b**) of OPN purified from human milk

It is important to note that when COM is precipitated from ultrafiltered urine containing purified mOPN, the protein is incorporated into the mineral, since it is present in the demineralised crystal extracts even after copious washing with water, which removes superficial protein from the COM crystal surface [43]. The demineralised extract of unwashed COM crystals precipitated from an aqueous solution of the same purified mOPN preparation also contains a band corresponding to the same molecular mass, but faint staining is also visible as a trail spanning the entire length of the lane, which corresponds to the extensive smear in the accompanying blot (lane 6). This again suggests that precipitation of COM crystals, per se, causes disruption and polymerisation of the mOPN molecule and its fragments, as mentioned above. However, when the crystals are washed with water, the band and smears disappear entirely (lane 7) indicating clearly that mOPN is not an intracrystalline component of inorganic COM crystals.

We cannot precisely explain the smearing observed in the gels and blots in Figs. 2 and 3, or why lanes 5 and 6 of the western blots in Fig. 3 do not contain discrete bands corresponding to those seen in the accompanying gels. OPN is well known to behave inconsistently during SDS-PAGE, with bands ranging from as low as 20–25 kDa to values as high as 80 kDa being reported, depending upon experimental conditions [12]. In addition to molecular fragmentation and polymerisation, as suggested above, possible reasons could include proteolysis, slow migration of heterogeneous forms of OPN caused by variable degrees of phosphorylation and glycosylation, or discrepancies

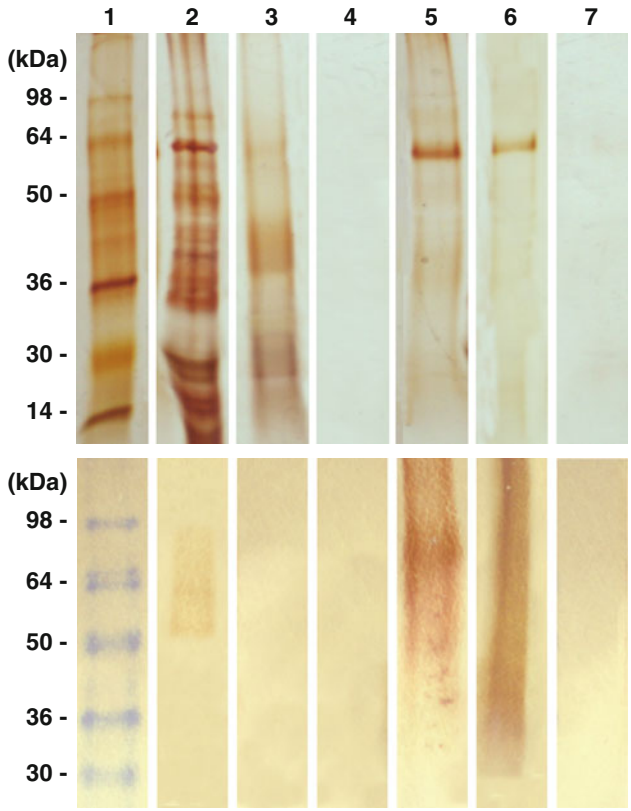

Fig. 3 SDS-PAGE gel (*top lanes*) and corresponding western blots stained for OPN (*bottom lanes*) of proteins from urine samples or demineralised COM crystals. All crystals were washed with water unless otherwise indicated. *Lane 1* standards, *lane 2* centrifuged and filtered urine (2 μg), *lane 3* crystals precipitated from centrifuged and filtered urine (3 μg), *lane 4* crystals precipitated from ultrafiltered urine (4 μg), *lane 5* crystals generated in ultrafiltered urine containing mOPN (4 μg), *lane 6* unwashed crystals deposited from an aqueous solution of mOPN (4 μg), *lane 7* washed crystals deposited from an aqueous solution of mOPN (4 μg). *Values in parentheses* show the amount of protein added to each lane. Loads for corresponding blots were one-fifth of those used for gel electrophoresis

between the mass and charge of the molecule, whose high acidity could also cause poor pairing with SDS. Unknown interferences during SDS-PAGE and western blotting may also account for the anomalous observations.

Control crystals

Figure 4 shows bright field and fluorescence confocal microscopy, and FESEM images of representative control crystals precipitated from UF urine and aqueous solutions in the absence of added OPN. The uCOM crystals are typical "coffin"-shaped crystals usually observed in human urine, while the iCOM crystals exhibit the common penetration-twinned monoclinic shape of inorganic COM [52]. Both uCOD and iCOD crystals show classical tetrahedral bipyramidal morphology. As expected, no fluorescence could be seen in any of the crystals.

uCOM crystals precipitated in the presence of mOPN

Unwashed crystals

Unwashed uCOM crystals precipitated in the presence of mOPN (Fig. 5), which are indistinguishable in size and shape from the corresponding control crystals (Fig. 4), fluoresce with intensity proportional to the concentration of mOPN. The fluorescence patterns at 0.5 and 1 mg/L suggest that mOPN, while distributed over the entire crystal surface, is concentrated towards the crystal centre, as has been previously noted [4, 53]. The bright field images indicate that the crystals are intact. Nonetheless, the FESEM image at 5 mg/L show topographical imperfections towards each end of the crystal, which are consistent with selective binding of the protein to the four end faces indicated in Fig. 1 [48]. FESEM images are not sharp, particularly at higher mOPN concentrations, probably because of the extraneous organic material associated with the crystals.

Crystals washed with water

The bright field, fluorescence and FESEM images (Fig. 6), all indicate that copious washing with water caused marked erosion of the crystals, which increased relative to mOPN concentration. The side faces and adjoining crystal regions appear relatively intact. However, FESEM examination of the top face at 0.1 mg/L shows more extensive degradation towards each end of the crystal, with pitting presenting as a bow–tie pattern suggestive of preferential binding of mOPN to the end faces [48]. This impression is also evident at higher concentrations, where the crystals are severely degraded; cleavage along the long axis and complete absence of their central regions probably resulted from the leaching of soluble mOPN from the crystal bulk. At the highest mOPN concentration, the ends of many crystals were frequently missing, as shown here, while the remnants resembled a bow–tie oriented perpendicular to the pattern of erosion shown at 0.1 mg/L. The interiors appear to comprise a mixture of discrete sub-crystalline particles of approximately 100–200 nm in size embedded in organic material, as has been previously observed in urinary COM crystals treated with protease [4, 54].

Crystals washed with 0.1 M NaOH

We have previously reported that uOPN is not incorporated into COM crystals precipitated from centrifuged and filtered urine [5], which is contrary to the observations described in the previous section with mOPN. We therefore also washed the crystals with 0.1 M NaOH, to remove any remnant protein attached to the COM crystal surfaces [6, 43]. This procedure also produced marked crystal erosion, which

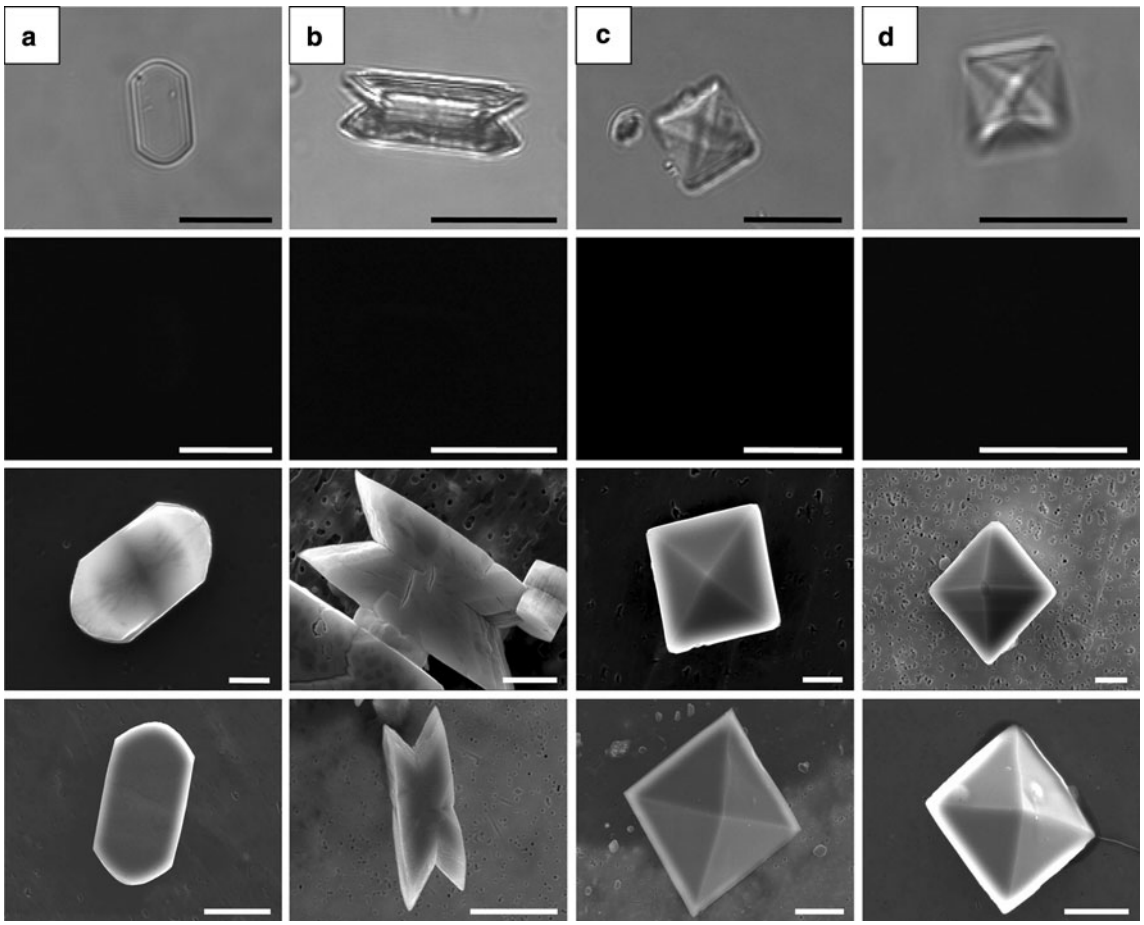

Fig. 4 Control crystals generated in the absence of added OPN. **a** uCOM crystal precipitated from UF urine, **b** iCOM crystals precipitated from aqueous solution, **c** uCOD crystal precipitated from UF urine, **d** iCOD crystal precipitated from aqueous solution. The *bottom row* shows representative crystals after washing with water. *Bar* on bright field and fluorescent images = 10 μm; *bar* on FESEM images = 2 μm

became more pronounced as the mOPN concentration increased, as shown in the bright field, fluorescence and FESEM images in Fig. 7. Again, numerous sub-crystalline particles are visible, but they are not immersed in organic material, which would have been removed by the alkali wash. As was seen with the water wash, the centres of many crystals are absent. Once again, pitting is distributed in a bow–tie pattern indicative of attachment of mOPN to the end faces. Although this is most evident in the scanning electron micrographs, it is also visible in the fluorescence images, especially at the highest mOPN concentration, where the greatest reduction in fluorescence corresponds to the most severely degraded regions of the crystals.

iCOM crystals precipitated in the presence of mOPN

Qiu et al. [38] reported that although OPN binds to the {100} face of iCOM, it is not included within the mineral. However, that study used pre-formed crystals, not crystals precipitated de novo in the presence of OPN, as occurred here. Diagrams were therefore prepared to assist with the interpretation of fluorescence patterns obtained for iCOM crystals precipitated in the presence of OPN. They show fluorescence patterns that would be expected after adsorption of OPN to different crystal faces and edges, followed by its interment into the mineral bulk (Fig. 8), as well as those that might result from adsorption of OPN molecules and their subsequent displacement to the crystal surfaces by COM mineral accumulating beneath them (Fig. 9). Note that in Figs. 10 and 11, the {010} faces are perpendicular to the plane of vision and are seen as the long parallel lines on each side of the crystals, while the four {121} faces, which are oblique to the {010} faces, are at each end of the crystals as shown in Fig. 1. It should be stressed that distributions could appear different when observed from the <100> or <121> directions.

Unwashed crystals

Figure 10 shows unwashed iCOM crystals generated from aqueous solutions of OPN, which, though morphologically

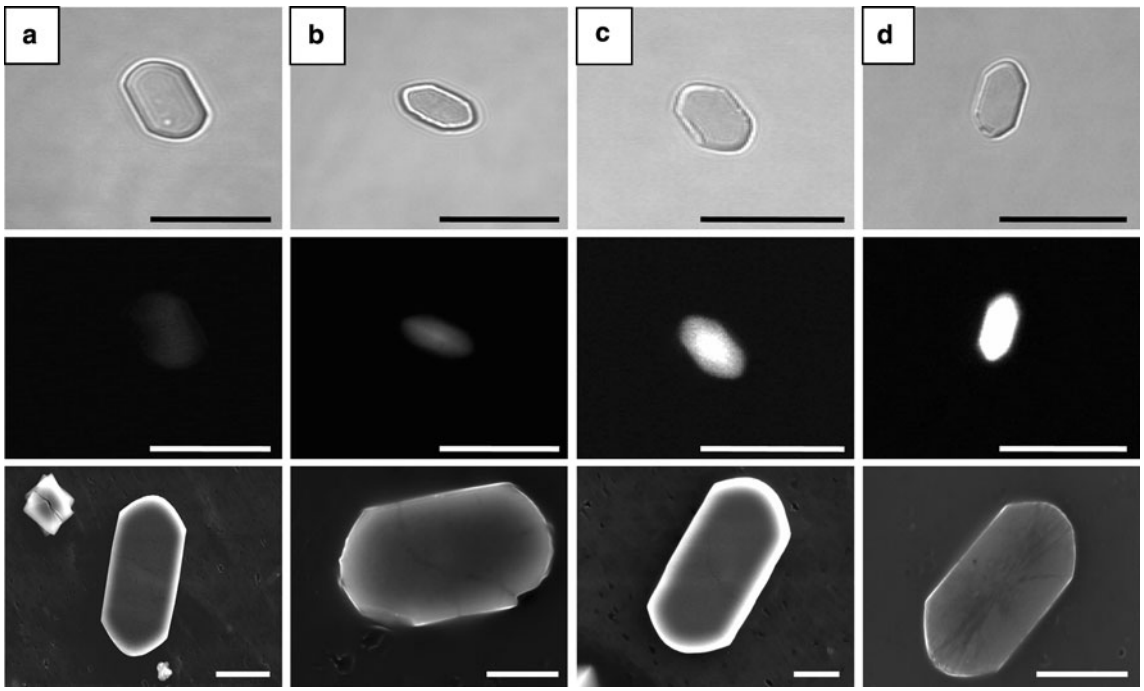

Fig. 5 Unwashed uCOM crystals precipitated from ultrafiltered urine containing increasing concentrations of OPN. **a** 0.1 mg/L, **b** 0.5 mg/L, **c** 1 mg/L, **d** 5 mg/L. *Bar* on bright field and fluorescent images = 10 μm; *bar* on FESEM images = 2 μm

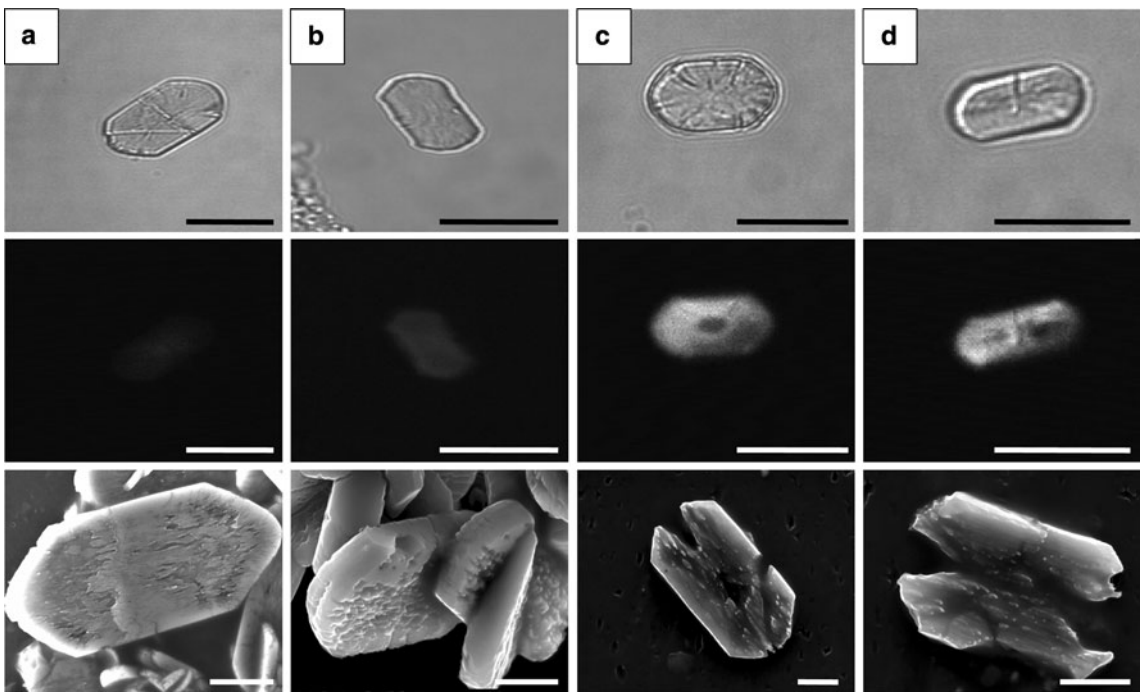

Fig. 6 uCOM crystals precipitated from ultrafiltered urine containing increasing concentrations of OPN, and washed with water. **a** 0.1 mg/L, **b** 0.5 mg/L, **c** 1 mg/L, **d** 5 mg/L. *Bar* on bright field and fluorescent images = 10 μm; *bar* on FESEM images = 2 μm

identical to their corresponding controls, have blotches on their {010} faces. As observed with the uCOM crystals, the intensity of fluorescence increases in proportion to the OPN concentration, being visible as a bow–tie pattern that could indicate incarceration of the protein within the mineral after selective binding to the {100} faces (Fig. 8, pattern 1) or to the edges between the {100} and {010} faces (Fig. 8, pattern 6). Alternatively, the bow–tie distribution could

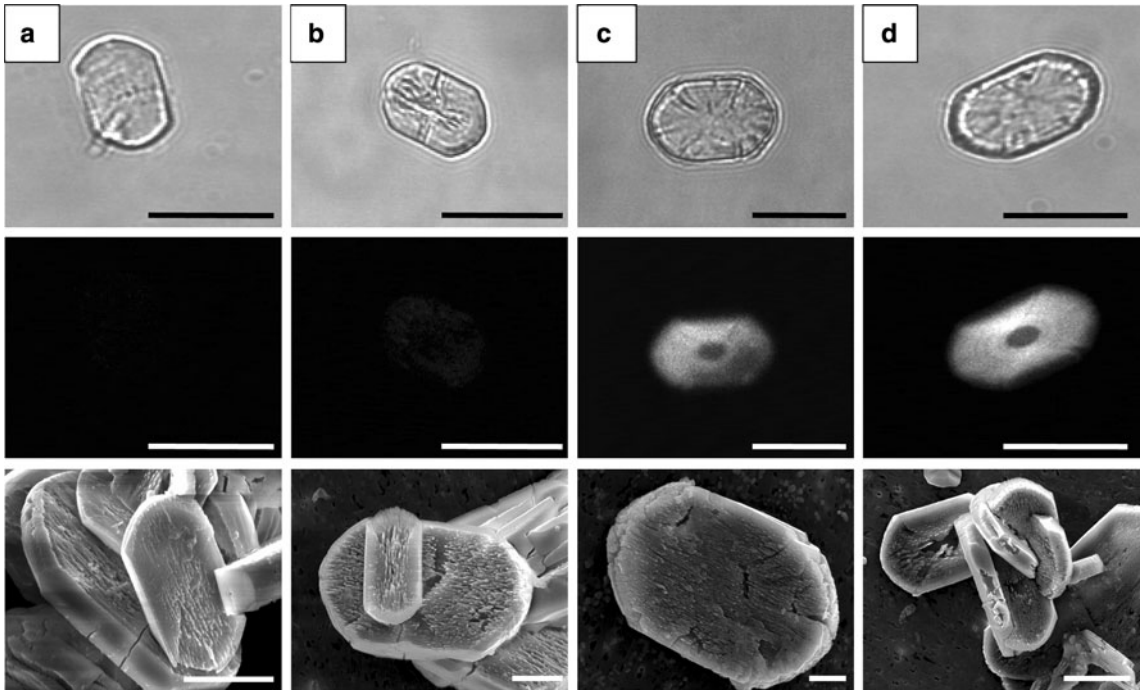

Fig. 7 uCOM crystals precipitated from ultrafiltered urine containing increasing concentrations of OPN, and washed with 0.1 M NaOH. **a** 0.1 mg/L, **b** 0.5 mg/L, **c** 1 mg/L, **d** 5 mg/L. *Bar* on bright field and fluorescent images = 10 μm; *bar* on FESEM images = 2 μm

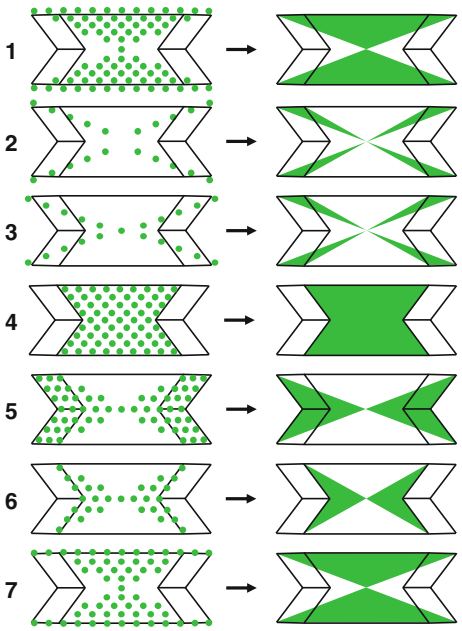

Fig. 8 Final fluorescence patterns expected after irreversible adsorption of OPN to successive layers of different faces and edges of iCOM crystals, and incorporation of the protein into the mineral bulk, viewed from the <010> direction. **1** Binding to (100) faces, **2** attachment to the {100} faces at the edges of intersection with the {121} planes, **3** attachment to the {121} faces at the edges of intersection with the {100} planes, **4** binding to the {010) faces, **5** attachment to the {121} faces, **6** attachment to the edges between the {010} and {121} faces, **7** attachment to {010} faces at the edges of intersection with the {100} faces

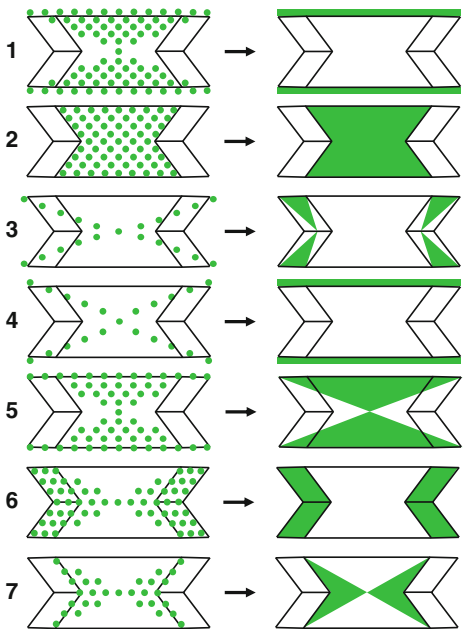

Fig. 9 Final fluorescence patterns expected following adsorption of OPN to successive layers of different faces and edges of iCOM crystals, and deposition of mineral ions beneath the adsorbed protein (that is, protein remains on the crystal surface), viewed from the <010> direction. **1** Binding to {100} faces, **2** attachment to {010} faces, **3** attachment to {121} faces at the edges of intersection with the {100} planes, **4** binding to the {100} faces at the edges of intersection with the {121} planes, **5** attachment to {010} faces at the edges of intersection with the {100} faces, **6** adsorption to {121} faces, **7** attachment to the edges between the {010} and {121} faces

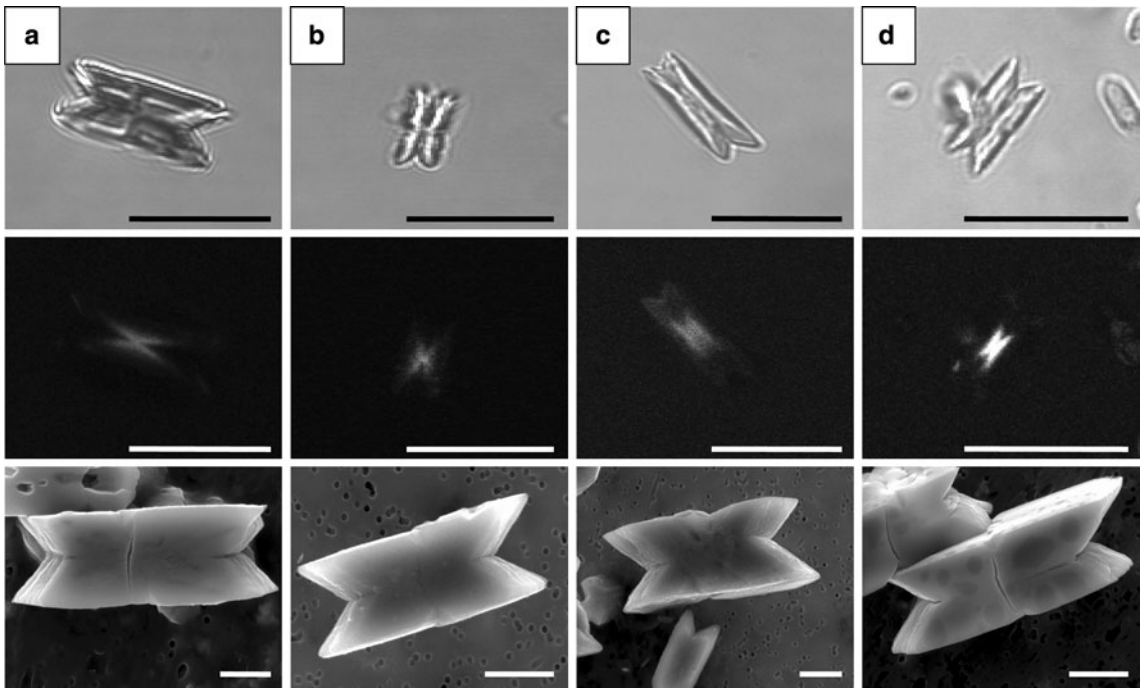

Fig. 10 Unwashed iCOM crystals precipitated from aqueous solutions containing increasing concentrations of mOPN. **a** 0.01 mg/L, **b** 0.05 mg/L, **c** 0.1 mg/L, **d** 0.5 mg/L. *Bar* on bright field and fluorescent images = 10 μm; *bar* on FESEM images = 2 μm

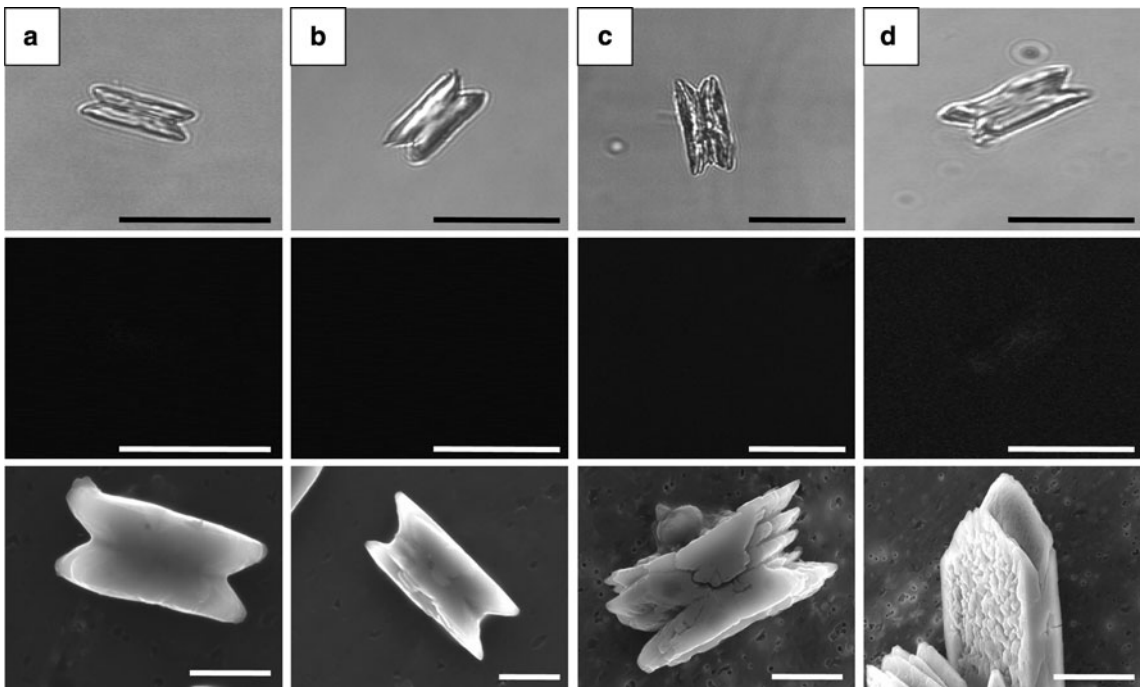

Fig. 11 iCOM crystals precipitated from aqueous solutions containing increasing concentrations of OPN, washed with water. **a** 0.01 mg/L, **b** 0.05 mg/L, **c** 0.1 mg/L, **d** 0.5 mg/L. *Bar* on bright field and fluorescent images = 10 μm; *bar* on FESEM images = 2 μm

result from adhesion of OPN to the {010} side of the junction of the {010} and {100} faces as the crystal enlarged by deposition of COM mineral beneath the adsorbed protein (Fig. 9, pattern 5). The fact that the fluorescence was concentrated at the crystal centres at low concentrations and did not extend to the crystal periphery

suggests that OPN was completely depleted from the surrounding solution as the crystals grew.

Washed crystals

Images of washed crystals are presented in Fig. 11. Although their general shapes are unaltered, significant pitting is seen on the {100} faces at the two highest concentrations and etching is also clearly visible on the {010} surfaces, particularly at the two highest OPN concentrations. Washing with water removed all fluorescence except for small vestiges that are barely visible, even at the highest OPN concentration. Removal of fluorescence suggests that most, if not all, of the protein had been located primarily upon the surface. It can be concluded, therefore, that OPN probably binds to the {010} side of the edge between the {010} and {100} faces (Fig. 9, pattern 5), which is in keeping with the marked erosion of the {010} face visible in the FESEM images, as well as on the {121} faces (FESEM image C), which would also have been affected. Nonetheless, binding to the {100} face may also have occurred, since the entire {100} face of the crystal generated at the highest OPN concentration (FESEM image D) is significantly etched: had binding occurred only at the {010}/{100} edges, pitting would have been expected to occur on the {100} face in a bow–tie arrangement extending across the crystal from one {010} face to the other.

Thus it is apparent that when iCOM crystals are precipitated from a highly supersaturated inorganic solution in the presence of OPN, the protein binds to the {100} face itself and also to the junction of the {100} and {010} faces. It is also apparent that mineral deposition occurs beneath or around the adsorbed protein, which is easily removed by washing with water, leaving large etch pits where its attachment has interrupted the continuity of mineral deposition.

Pre-formed iCOM crystals coated with mOPN in PBS and ultrafiltered urine

To enable comparison with results of published studies, pre-formed iCOM crystals were coated with OPN at a final concentration of 0.5 mg/L in PBS and in UF urine (pH 6.1) at final calcium concentrations of 2 and 8 mM. In PBS (Fig. 12a), faint fluorescence can be seen along the two {100} faces, which is concentrated slightly more intensely at the intersections of the {100} and {121} faces, being visible as two bright spots at both ends of the crystal. This pattern is repeated with greater intensity in UF urine at a calcium concentration of 2 mM (Fig. 12b), and even greater intensity at 8 mM calcium (Fig. 12c). Although not quantitative, the results suggest that OPN binds more strongly to iCOM crystals in UF urine than in PBS, and at higher calcium concentrations than lower.

Pre-formed atypical iCOM crystals coated with OPN in PBS

Direct binding of OPN to iCOM crystals in UF urine containing OPN (0.5 mg/L) was also examined using pre-formed crystals with atypical morphology [51] in order to enable direct observation of different crystal faces oriented horizontally to the observer. In Fig. 13a, fluorescence appears to be present on the $\{\bar{1}21\}$ and $\{12\bar{1}\}$ faces, as well as on the $\{02\bar{1}\}$ and {021} faces, with intensity being greatest along the external crystal edges. Less intense fluorescence is also apparent as lines corresponding to the {100} and $\{\bar{1}00\}$ faces. This selectivity is repeated on the crystal shown in Fig. 13b, where fluorescence appears most obvious on the $\{0\overline{21}\}$ face, but is also seen on the $\{12\bar{1}\}$ and {100} faces. No fluorescence is visible on the predominant $\{1\overline{21}\}$ face or adjacent {010} surface. Faint fluorescence in Fig. 13c is seen principally on the {021}

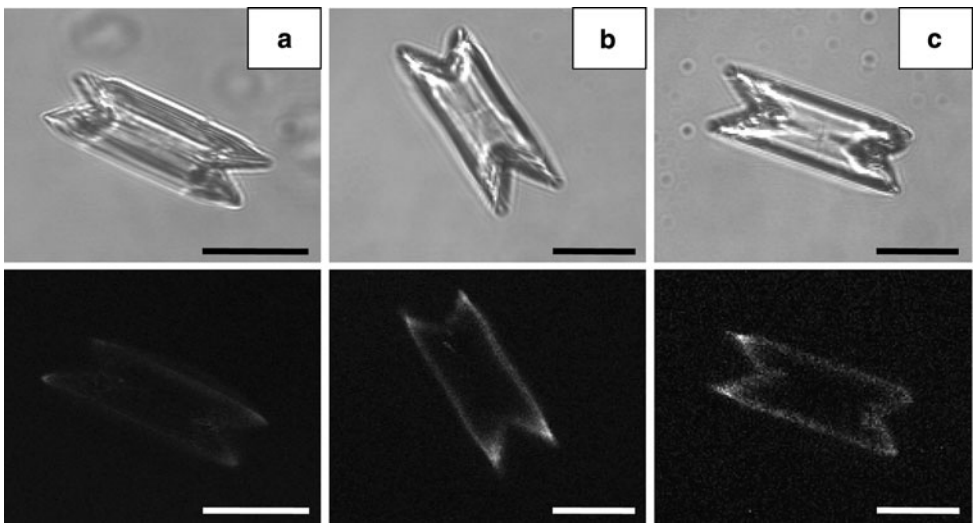

Fig. 12 Pre-formed iCOM crystals superficially coated with OPN (0.5 mg/L) in PBS (**a**) and in ultrafiltered urine at calcium concentrations of 2 mM (**b**) and 8 mM (**c**). *Scale bar* represents 10 μm

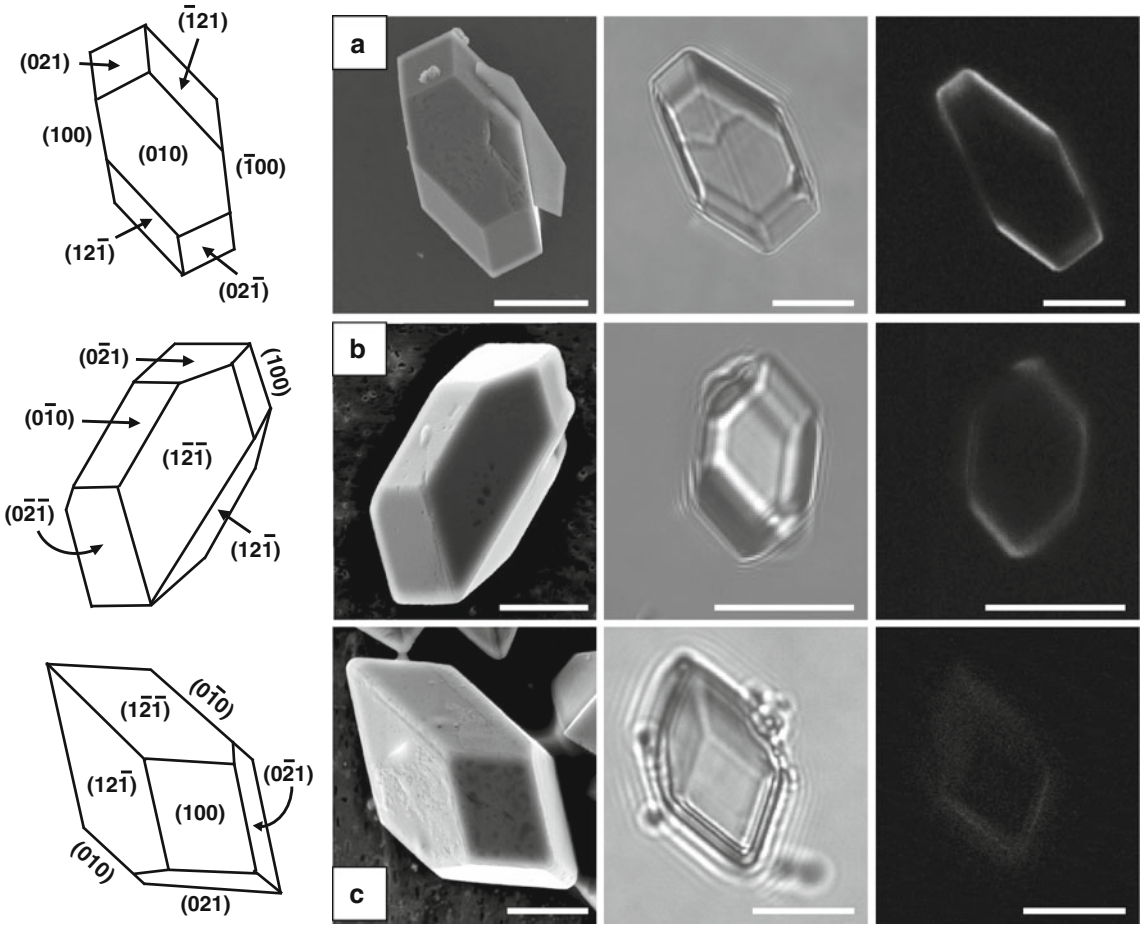

Fig. 13 Atypical COM crystals, prepared according to Jung et al. [47] and Sheng et al. [56], to enable direct observation of COM crystals with {010}, {121} or {100} faces oriented horizontally to the observer

and {0$\bar{2}$1} faces. Significant direct binding of OPN to the {010} and {100} faces is not seen.

uCOD crystals precipitated in the presence of OPN

Unwashed crystals

Figure 14 shows unwashed COD crystals precipitated from UF urine in the presence of increasing concentrations of purified OPN. Once again, the intensity of fluorescence appears to increase in proportion to OPN concentration, being visible in equal strength on each equivalent {101} face of the COD crystal and suggesting that OPN binds with equal affinity to each. Nonetheless, at OPN concentrations of 0.5 mg/L and higher, more intense fluorescence can be seen in the form of a cross corresponding to the common edges of adjacent {101} faces, suggesting preferential binding of the protein to those points. At all OPN concentrations, attached to the larger COD crystals are COM crystals that probably formed as secondary nucleants during preparation of the COD crystals and which are most apparent in the FESEM images. These COM crystals continue to fluoresce after washing, indicating incorporation of OPN into the crystal structure, as shown in Figs. 6 and 7.

Washed crystals

Washing of the uCOD crystals with water had little apparent influence on the distribution or intensity of fluorescence, which again increased relative to OPN concentration (Fig. 15). Persistence of the same pattern of fluorescence as shown in Fig. 14 indicates that OPN is intracrystalline. Superficial pitting at the two highest OPN concentrations, particularly at 5 mg/L, suggests that leaching of the protein from within the mineral structure occurred during the washing procedure.

iCOD crystals precipitated in the presence of OPN

Unwashed crystals

Shown in Fig. 16 are iCOD crystals precipitated from aqueous solutions of OPN, which again exhibit an apparent

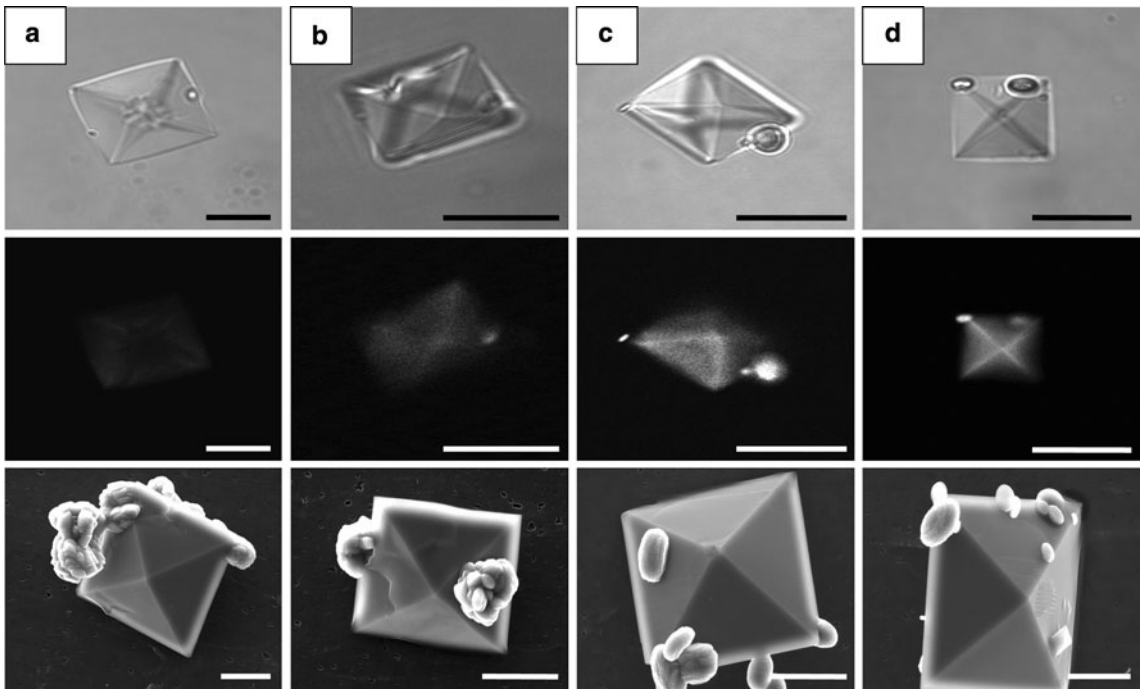

Fig. 14 Unwashed uCOD crystals precipitated from ultrafiltered urine containing increasing concentrations of purified OPN. **a** 0.1 mg/L, **b** 0.5 mg/L, **c** 1 mg/L, **d** 5 mg/L. *Bar* on bright field and fluorescent images = 10 μm; *bar* on FESEM images = 5 μm

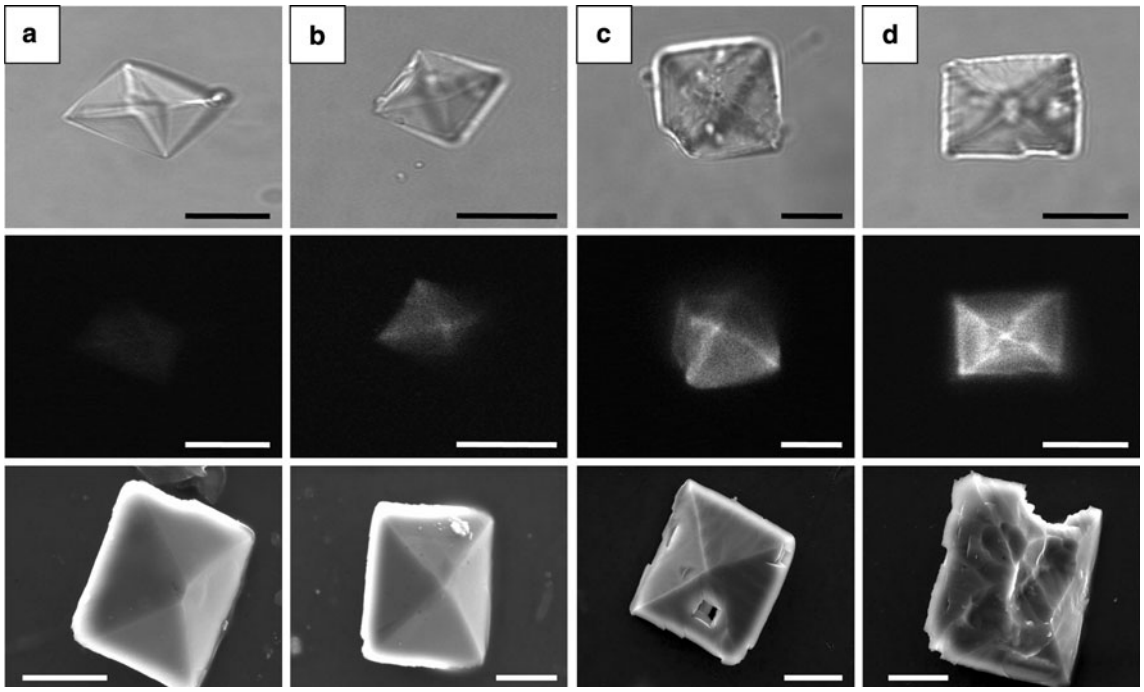

Fig. 15 uCOD crystals precipitated from ultrafiltered urine containing increasing concentrations of purified OPN, washed with water. **a** 0.1 mg/L, **b** 0.5 mg/L, **c** 1 mg/L, **d** 5 mg/L. *Bar* on bright field and fluorescent images = 10 μm; *bar* on FESEM images = 5 μm

direct relationship between fluorescence strength and increasing OPN concentration. No fluorescence is obvious at the lowest OPN concentration, and at the other concentrations it is fainter than those observed in the uCOD crystals. This difference can perhaps be attributed to the lower OPN concentrations used in preparation of the iCOD crystals. As occurred with the uCOD crystals, the protein seemed to bind with equal affinity to all faces of the iCOD

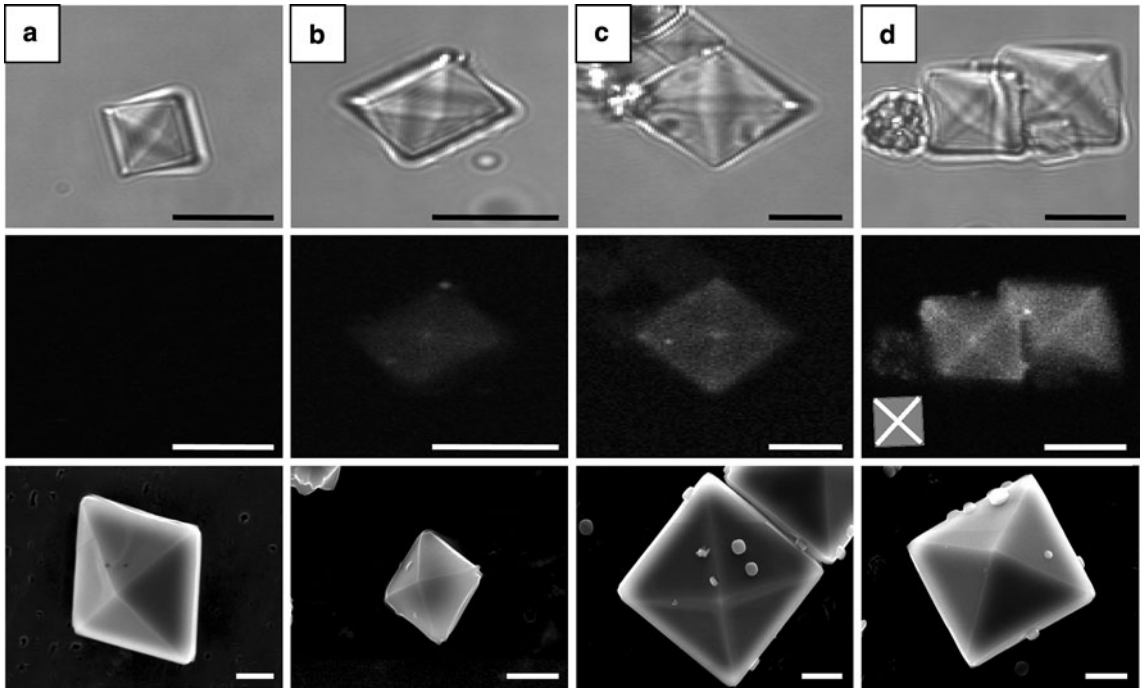

Fig. 16 Unwashed iCOD crystals precipitated from aqueous solutions containing increasing concentrations of purified OPN. **a** 0.01 mg/L, **b** 0.05 mg/L, **c** 0.1 mg/L, **d** 0.5 mg/L. In the right hand image in column **d** is shown a cartoon representing the observed fluorescence pattern. *Bar* on bright field and fluorescent images = 10 μm; *bar* on FESEM images = 2 μm

crystal, with some concentration in intensity along the intersections of contiguous {101} faces, which is most obvious at the highest OPN concentration. Some secondary COM nucleants can be seen attached to the COD crystals, which exhibit normal urinary COM morphology.

Washed crystals

No fluorescence was detectable in iCOD crystals precipitated at the two lowest OPN concentrations (Fig. 17), suggesting that the faint fluorescence observed in the unwashed iCOD crystal (Fig. 16b) can be ascribed to mOPN present upon the crystal surface, which was removed by washing. At the two highest OPN concentrations washing changed the fluorescence pattern from a square extending to the 4 {110} outer rims, as shown in Fig. 16, to a 4-pointed star corresponding to the upper 4 adjoining {101}/{101} edges, suggesting that some of the protein had been only superficially attached to the {101} faces. However, the persistence of fluorescence after washing confirms that OPN is incarcerated inside the mineral bulk, in a distribution pattern consistent with principal binding of the protein to the edges between adjacent {101} faces. Small secondary COM nucleants are again visible, which retain their fluorescence after washing, as noted above. A small amount of crystal degradation is apparent in FESEM image D, congruent with removal by the washing procedure of small amounts of intracrystalline OPN close to the crystal surface.

Discussion

Urine protein fractions [35] and certain urinary proteins [55, 56] modulate COM crystal growth, aggregation, and/or adhesion to cultured renal cells, and intracrystalline proteins have been shown to facilitate the degradation and dissolution of crystals within cells [57, 58], all of which depend upon attachment of the proteins to the crystal surfaces. Investigating the distribution of individual proteins upon or within COM crystals has the potential to yield valuable clues about factors that influence interactions between them, and thus provide a rational basis for the design and synthesis of peptides possessing specific molecular motifs that could form the basis of future prophylactic stone therapy.

Using various techniques, several authors have studied the binding patterns of OPN peptides [39–41, 59] or different isoforms of OPN derived from a variety of biological sources [22, 38, 39] to pre-formed COM crystals. Others have precipitated COM crystals in the presence of OPN isoforms [21, 22] or OPN peptides possessing different degrees of phosphorylation [40, 41]. A recent study used a constant composition method combined with molecular modelling to measure the inhibitory effects of an OPN peptide on COM crystallisation and to determine the binding specificity of the peptide [59]. Thus, to date, there have been no investigations of face-specific attachment of OPN to pre-formed COM crystals in human urine, or inclusion of

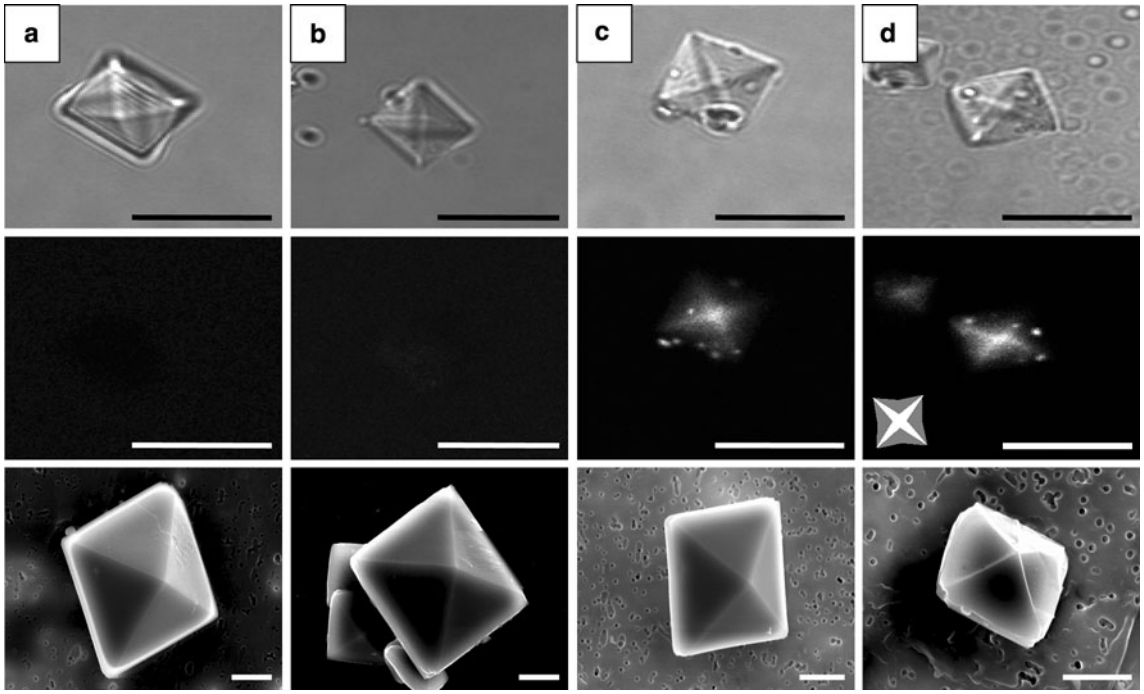

Fig. 17 iCOD crystals precipitated from aqueous solutions containing increasing concentrations of purified OPN, and washed with water. In the right hand image in column **d** is shown a cartoon representing the observed fluorescence pattern. **a** 0.01 mg/L, **b** 0.05 mg/L, **c** 0.1 mg/L, **d** 0.5 mg/L. *Bar* on bright field and fluorescent images = 10 μm; *bar* on FESEM images = 2 μm

the protein into COM or COD crystals precipitated from human urine. In this study we used a combination of SDS-PAGE, western blotting, confocal fluorescence microscopy and FESEM to assess the face-specific binding of highly phosphorylated human milk OPN to preformed urinary and inorganic COM and COD crystals, as well as its incorporation into COM and COD crystals generated de novo from urine and aqueous inorganic solutions.

As we have reported previously, at a calcium concentration of 2 mMol/L uOPN was undetectable by western blotting in demineralised extracts of COM crystals precipitated from centrifuged and filtered urine [5]. On the other hand, mOPN was clearly evident in both gels and blots of extracts of washed crystals precipitated from UF urine containing mOPN, confirming that it is incorporated into the uCOM mineral bulk.

There are several possible explanations for this discrepancy.

1. *Differences in phosphorylation* Human milk OPN possesses 36 phosphorylation sites [14, 22]. OPN in human urine contains only 8 phosphate groups, along with fragments that possess around 6 phosphate moieties [60]. Since OPN's phosphate complement influences its relative adsorption to the various faces of the COM crystal [22], apparently through non-specific electrostatic interaction between its phosphate groups and Ca^{2+} ions of the crystal surface [21], the failure of human uOPN to incorporate into COM crystals generated in urine, in contrast to the ability of mOPN to do so, could be a function of its low level of phosphorylation.
2. *Differences in homogeneity* The mOPN used in this study was relatively homogeneous, while the urinary form was very heterogeneous, as shown by their respective migration patterns on SDS-PAGE and western blotting analysis. Human urine contains a broad range of OPN isoforms comprising the full-length protein and truncated forms lacking the C-terminal region Leu229/Lys231–Asn298 [60], as well as polymeric species with Mr values as high as 80 kDa and segments with molecular masses as low as 20-25 kDa [12, 45] that probably represent products of endogenous serine protease activity [44] or storage [45]. Like their parent [15], these OPN fragments are highly flexible, a molecular feature that alters their steric configurations and influences their ability to bind to cells and receptors [61] and undoubtedly, therefore, their crystal binding properties.
3. *Differences in calcium-binding domains* Human milk and urinary OPN may differ with regard to the integrity of their acidic poly-Asp calcium-binding domains [62] or other multiple putative Ca^{2+} binding motifs that are known to affect the OPN molecule's affinity for hydroxyapatite crystals [12, 63], and perhaps, therefore, its ability to attach to CaOx.

4. *Competition from other urinary proteins* mOPN appeared to bind preferentially to the end faces of crystals precipitated from UF urine, which contained no macromolecules larger than 10 kDa in mass. Since prothrombin fragment (PTF1) and human serum albumin (HSA) also bind to those faces [48], the absence of uOPN from crystals generated in CF urine [5] may result from its inability to compete successfully with those proteins for limited binding sites on the end surfaces. This possibility is strengthened by observations with HSA and PTF1. HSA attaches to the end faces of COM in UF urine. However, in UF urine containing added PTF1, HSA attaches to the end faces only after all PTF1, which also binds preferentially to those faces, has been exhausted from solution [48]. An analogous argument could also be used to explain the virtual absence of PTF1 from urinary COD crystals, to which uOPN prefers to bind [5].

Differences were also observed between iCOM and uCOM crystals precipitated in the presence of OPN. Western blots confirmed the presence of intracrystalline mOPN in washed and unwashed uCOM crystals. However, fluorescent mOPN associated with iCOM crystals was completely removed by washing, demonstrating that the protein had been only superficially associated with the crystal surface. Nonetheless, in both cases the mOPN appeared to have undergone major fragmentation and polymerisation, as shown by extensive smearing of the western blot pattern over a large range of molecular masses. Breakage of internal bonds and total molecular dissociation, as well as catalytic action that can modify conformation and composition, are known to result from formation of multiple bonds between proteins and surfaces, even if they are eventually uncoupled [64].

Numerous studies have reported the effects of OPN or model OPN peptides on the crystallisation of HA eg, [19, 23, 62, 65, 66] and CaOx e.g., [11, 16, 17, 21, 32, 59, 67–69]. However, recent studies have concentrated on face-specific interactions between COM crystals and segments of the OPN molecule [41], or OPN itself, derived from various sources [21, 22, 38–40, 68, 70], using a variety of techniques.

The bow–tie pattern of mOPN fluorescence in unwashed iCOM crystals was consistent with selective binding of the protein either to the {100} faces or to the edges between the {100} and {010} faces, followed by its inclusion into the growing structure. However, the same pattern could also have resulted from irreversible binding of the mOPN to the edges between the {100} and {010} faces. To demonstrate unambiguous incorporation of a protein into a mineral structure, it is imperative that all extraneous material adsorbed to the crystal surface is scrupulously removed [43]. Thorough washing of the crystals with water completely removed visible fluorescence at all but the highest OPN concentration, where it was barely detectable. This finding was consistent with our inability to detect OPN by western blotting in extracts of washed iCOM crystals, as well as our previous demonstration that incorporation of uOPN into COM crystals precipitated from urine was undetectable at 2 mM calcium [5], which is the concentration at which the uCOM crystals used in the present study were generated. In contrast, Hunter et al. [22] reported incorporation of bone OPN into iCOM crystals in a cross pattern indicative of preferential adsorption to the {100}/{121} edges, as shown in patterns 2 and 3 of our Fig. 8. However, the faintness of the signal detected by Hunter et al. [22], coupled with the absence of significant fluorescence at the crystal centre, suggests that the attraction of bOPN for the growing iCOM crystal surface, like that of mOPN demonstrated in this study, is relatively minor. Their detection of small quantities of intracrystalline bone OPN is possibly attributable to their use of OPN at a concentration double that used in the present study.

Although mOPN did not incorporate to any significant extent into the iCOM mineral structure, it apparently attached to the crystal surface, as indicated by marked erosion on the {010} and {100} faces, which suggested superficial attachment of mOPN, predominantly to the {010} side of the edge between the {010} and {100} faces. However, direct binding to the {100} face also appeared to occur, since the entire surfaces of those faces at the highest OPN concentration were significantly etched. This strongly suggests that during growth of the crystals, laying down of fresh solute occurred beneath or around the adsorbed protein, whose attachment caused discontinuities in mineral deposition, visible as large etch pits after washing with water. Such attachment, but not incorporation of OPN is consistent with observations of Qiu et al. [38]. Those authors showed, using atomic force microscopy, that although OPN attached to terraces on the {100} face, it was not subsumed by the advancing growth front, which progressed unhindered beneath the adsorbed protein. They attributed this phenomenon to insufficient height on the steps to accommodate the molecule.

Our results showed that when iCOM was precipitated from aqueous solutions containing mOPN, the protein apparently attached predominantly to the {010} side of the edge between the {010} and {100} faces, but also to the {021} faces, which were considerably eroded by washing. However, the same binding preferences were not reproduced exactly when pre-formed iCOM crystals were incubated in PBS or in UF urine. In PBS, direct binding to the {010} face did not seem to occur, since it was never uniformly covered with fluorescence. The fluorescence distribution was consistent with weak binding of mOPN to

the {100}/{010} edges and {121} faces, but stronger attachment to the end tips of the crystals, that is, to the points of intersection of the {100} and {121} faces. This pattern was identical to that reported by Hunter and his colleagues for several OPN preparations derived from different sources [22, 39, 68] and for a range of highly phosphorylated, and aspartic acid- or glutamic acid-rich synthetic peptide sequences of OPN [40]. However, because the {100} and {121} faces were always viewed perpendicularly or obliquely, we were unable to decide unambiguously whether binding had occurred directly to those faces.

One limitation of assessing binding selectivity from fluorescence distributions viewed from only one aspect is that fluorescence intensity and pattern can be distorted by the grazing angle of the incident beam. Thus, unless a molecule binds to a face oriented horizontally to the microscope, it is difficult to conclude whether attachment has occurred to a specific crystal face or to its junction with a contiguous face. In an attempt to overcome this problem, iCOM crystals with atypical morphologies were prepared [51, 70], which enabled observation of different crystal faces presented directly to the observer. Using this approach, all three morphologies exhibited fluorescence patterns consistent with strongest adhesion to the {121} faces, with less binding to the {021} faces and minor attachment to the junction of the {100} and {010} faces. However, when those faces were horizontally oriented with the plane of examination, none appeared uniformly covered with fluorescence, suggesting that the observed patterns must have resulted principally, if not entirely, from binding to common edges of those faces.

We are unable to offer a plausible explanation for the discrepancies between the fluorescence distributions of the atypical and more commonly observed iCOM crystal morphologies, or between our findings and those of Qiu et al. [38], who reported the binding of uOPN principally to the {010} faces of growing crystals, on which occurred the most marked morphological modifications and strongest concentration-dependent inhibition of growth. Moreover, although our results are congruous with some binding of human mOPN to the {100} face, they differ from those of Langdon et al. [21] whose results indicated that bovine mOPN bound most avidly to that face. Differences between the binding preferences of human and bovine mOPN may reflect genetic molecular inconsistencies such as might explain disparities between the binding preferences of OPN from bovine milk and rat bone [21].

In order to assess the potential influence of other urinary constituents on the binding of mOPN, pre-formed iCOM crystals were also treated with ultrafiltered urine containing the protein. Here, the distribution of fluorescence appeared identical to that observed for crystals incubated in PBS, namely, along the {100}/{010} and {100}/{021} edges, but with greatest intensity at the {100}/{121} tips of the crystals. Of interest was the observation that fluorescence was apparently greater in UF urine than in PBS. Although not quantitative, the finding suggests that one or more unidentified urinary constituent(s) <10 kDa in mass may be able to mediate binding of the protein to the crystal surface. Measurement of uOPN levels by ELISA is known to be susceptible to the presence of unknown urinary components, and also to alter with changes in ambient calcium concentration [46], possibly because both affect the steric configuration of the protein's antibody-binding domains. Greater binding of uOPN to both COM and COD urinary crystals is also known to occur at higher urinary calcium concentrations [5], perhaps because calcium concentrations of 1–2 mM occupy only ~25 of the 50 potential calcium-binding sites of OPN [12], which are saturated at concentrations between 5 and 10 mM [71].

Prima facie, the distribution of fluorescence in COM crystals precipitated from UF urine in the presence of OPN was suggestive of binding to the top face. This was supported by FESEM examination of crystals washed with water or dilute alkali, which showed extensive erosion of the top face, particularly in the central portion. However, FESEM also revealed significant erosion in the form of a bow–tie shape extending from both ends of the crystals, which is congruent with binding to the end faces, as has been reported for PTF1 [48]. Both erosion patterns have been formerly observed in urinary COM crystals treated with protease [53, 54], or after attachment to Madin Darby canine kidney cells [57, 58]. Washing with water and dilute NaOH caused significant crystal degradation, the extent of which was apparently directly proportional to the concentration of mOPN. At the two highest concentrations, washing completely removed the crystal centres and ends, which was obvious from both the fluorescence patterns and FESEM images. Nonetheless, the remaining intact regions of the crystals continued to fluoresce strongly, indicating that the OPN was incarcerated within the mineral. The results of water and NaOH washing suggested that mOPN binds preferentially to the end faces of COM crystals precipitated from UF urine containing the protein and is incorporated into the mineral structure, thus confirming the SDS-PAGE and western blotting results shown in lane 5 of Fig. 3.

The incorporation of mOPN into uCOM crystals contrasts with its absence from iCOM crystals. This disparity is probably not attributable to differences in final ambient calcium concentrations between the methods used to prepare each crystal type, which were 2 (uCOM) and 2.5 mmol/L (iCOM). Furthermore, since other macromolecules >10 kDa had been removed from the UF urine in which the crystals were precipitated, inclusion of the

protein into uCOM crystals appears to have been facilitated by one or more unidentified low Mr (<10 kDa) macromolecular components of the UF urine or ionic constituents not present in the aqueous solutions in which the iCOM crystals were generated. It is noteworthy that the morphology of the uCOM crystals was unaffected by OPN, which has been shown to encourage the formation of dumbbell-shaped crystals from inorganic solutions [22, 41] and is hypothesised to be responsible for the occurrence of similarly shaped COM crystals in human urine [39].

Unlike that of COM, the binding of mOPN to both iCOD and uCOD was relatively straightforward and easily interpreted. Except at the lowest mOPN concentration, in the iCOD crystals, under both inorganic and urinary conditions, concentration-dependent fluorescence was visible on all the equivalent triangular {101} faces of the unwashed crystals, irrespective of whether they were precipitated from solutions containing the protein or were incubated in them after formation. In all instances, the fluorescence appeared to be concentrated along the spines between adjoining {101} faces. Washing with water had little, if any, effect on either the pattern or intensity of fluorescence associated with the uCOD crystals, indicating that the protein was incorporated into the mineral bulk. However, mOPN bound to the {101} faces of the iCOD crystals seemed reduced after washing, particularly around the square rim of the relatively undeveloped {100} faces. The 4-pointed star pattern that remained after washing, as opposed to the cross-within-a-square pattern in the unwashed crystals suggested that some of the mOPN may have been superficially attached to the {101} faces, but that most had remained incarcerated within the crystal along the {101}/{101} rims.

To our knowledge, face-specific interactions between OPN and COD crystals have been reported in only one paper [37], which investigated the inclusion of bovine milk OPN and its poly-Asp86–93 peptide into iCOD crystals and their effects on crystal morphology in aqueous media. Both the OPN and peptide produced enlargement of the {110} faces of COD crystals prepared from aqueous solutions, consistent with their attachment to those faces, together with consequent inhibition of growth. Intersectoral zoning of the fluorescent-tagged peptide inside the crystals was observed, confirming its incorporation into the mineral phase, but the study did not investigate whether the full-length bovine mOPN was incorporated into the iCOD crystals. Urinary COD crystals were also prepared in that study, but were used only to confirm, using SDS-PAGE and Western blotting, incorporation of urinary OPN into the mineral phase.

In this paper, we have described the first systematic examination of the face-specific binding of a full-length, highly phosphorylated human OPN molecule to COM and COD crystals precipitated from aqueous solutions and undiluted ultrafiltered human urine. We have shown that the patterns of interaction between OPN and calcium oxalate differ depending upon the anatomical and genetic source of the protein, and whether the crystals are (1) COM or COD; (2) generated in inorganic solutions or ultrafiltered human urine, or (3) pre-formed and coated with the protein or are precipitated in its presence. Taken together, our observations emphasise the need for circumspection when drawing conclusions about stone formation from data generated under inorganic conditions.

Acknowledgments The authors are indebted to Dr Jennifer Clarke for assistance with the confocal microscopy and to Dr Roger Qiu of the Lawrence Livermore National Laboratory, USA, for invaluable advice regarding the labelling of urinary COM crystal faces. Support from the National Institute of Diabetes and Digestive and Kidney Diseases (Grant 1R01-DK-064050-01A1) is gratefully acknowledged.

References

1. Addadi L, Weiner S (1985) Interactions between acidic proteins and crystals: stereochemical requirements in biomineralization. Proc Natl Acad Sci USA 82:4110–4114
2. Addadi L, Weiner S, Geva M (2001) On how proteins interact with crystals and their effect on crystal formation. Z Kardiol 90:92–98
3. Weiner S, Addadi L (1991) Acidic macromolecules of mineralized tissues: the controllers of crystal formation. Trends Biochem Sci 16:252–256
4. Fleming DE, van Riessen A, Chauvet MC, Grover PK, Hunter B, van Bronswijk W, Ryall RL (2003) Intracrystalline proteins and urolithiasis: a synchrotron X-ray diffraction study of calcium oxalate monohydrate. J Bone Min Res 18:1282–1291
5. Ryall RL, Chauvet MC, Grover PK (2005) Intracrystalline proteins and urolithiasis: a comparison of the protein content and ultrastructure of urinary calcium oxalate monohydrate and dihydrate crystals. BJU Int 96:654–663
6. Doyle IR, Ryall RL, Marshall VR (1991) Inclusion of proteins into calcium oxalate crystals precipitated from human urine: a highly selective phenomenon. Clin Chem 37:1589–1594
7. Merchant M, Cummins T, Wilkey D, Salyer S, Powell D, Klein J, Lederer E (2008) Proteomic analysis of renal calculi indicates an important role for inflammatory processes in calcium stone formation. Am J Physiol Renal Physiol 295:F1254–F1258
8. McKee MD, Nanci A, Khan SR (1995) Ultrastructural immunodetection of osteopontin and osteocalcin as major matrix components of renal calculi. J Bone Min Res 10:1913–1929
9. Tawada T, Fujita K, Sakakura T, Shibutani T, Nagata T, Iguchi M, Kohri K (1999) Distribution of osteopontin and calprotectin as matrix protein in calcium-containing stone. Urol Res 27:238–242
10. Hoyer JR, Otvos L, Urge L (1995) Osteopontin in urinary stone formation. Ann N Y Acad Sci 760:257–265
11. Kleinman JG, Wesson JA, Hughes J (2004) Osteopontin and calcium stone formation. Nephron Physiol 98:43–47
12. Denhardt DT, Guo X (1993) Osteopontin: a protein with diverse functions. FASEB J 7:1475–1482
13. Wang L, Qiu SR, Zachowicz W, Guan X, De Yoreo JJ, Nancollas GH, Hoyer JR (2006) Modulation of calcium oxalate crystallization by linear aspartic acid-rich peptides. Langmuir 22:7279–7285

14. Christensen B, Nielsen MS, Haselmann KF, Petersen TE, Sørensen ES (2005) Post-translationally modified residues of native human osteopontin are located in clusters: identification of 36 phosphorylation and five o-glycosylation sites and their biological implications. Biochem J 390:285–292
15. Fisher LW, Torchia DA, Fohr B, Young MF, Fedarko NS (2001) Flexible structures of SIBLING proteins, bone sialoprotein, and osteopontin. Biochem Biophys Res Commun 280:460–465
16. Shiraga H, Min W, VanDusen WJ, Clayman MD, Miner D, Terrell CH, Sherbotie JR, Foreman JW, Przysiecki C, Neilson EG, Hoyer JR (1992) Inhibition of calcium oxalate crystal growth in vitro by uropontin: another member of the aspartic acid-rich protein superfamily. Proc Natl Acad Sci USA 89:426–430
17. Worcester EM, Blumenthal SS, Beshensky AM, Lewand DL (1992) The calcium oxalate crystal growth inhibitor protein produced by mouse kidney cortical cells in culture is osteopontin. J Bone Min Res 7:1029–1036
18. Boskey AL, Maresca M, Ullrich W, Doty SB, Butler WT, Prince CW (1993) Osteopontin-hydroxyapatite interactions in vitro: inhibition of hydroxyapatite formation and growth in a gelatine-gel. Bone Miner 22:147–159
19. Hunter GK, Hauschka PV, Poole AR, Rosenberg LC, Goldberg HA (1996) Nucleation and inhibition of hydroxyapatite formation by mineralized tissue proteins. Biochem J 317:59–64
20. Saavedra RA (1994) The roles of autophosphorylation and phosphorylation in the life of osteopontin. Bioessays 16:913–918
21. Langdon A, Wignall GR, Rogers K, Sørensen ES, Denstedt J, Grohe B, Goldberg HA, Hunter GK (2009) Kinetics of calcium oxalate crystal growth in the presence of osteopontin isoforms: an analysis by scanning confocal interference microscopy. Calcif Tissue Int 84:240–248
22. Hunter GK, Grohe B, Jeffrey S, O'Young J, Sørensen ES, Goldberg HA (2009) Role of phosphate groups in inhibition of calcium oxalate crystal growth by osteopontin. Cells Tissue Org 189:44–50
23. Gericke A, Qin C, Spevak L, Fujimoto Y, Butler WT, Sørensen ES, Boskey AL (2005) Importance of phosphorylation for osteopontin regulation of biomineralization. Calcif Tissue Int 77:45–54
24. de Bruijn WC, de Water R, van Run PR, Boevé ER, Kok DJ, Cao LC, Romijn HC, Verkoelen CF, Schröder FH (1997) Ultrastructural osteopontin localization in papillary stones induced in rats. Eur Urol 32:360–367
25. de Water R, Noordermeer C, van der Kwast TH, Nizze H, Boevé ER, Kok DJ, Schröder FH (1999) Calcium oxalate nephrolithiasis: effect of renal crystal deposition on the cellular composition of the renal interstitium. Am J Kidney Dis 33:761–771
26. de Water R, Noordermeer C, Houtsmuller AB, Nigg AL, Stijnen T, Schröder FH, Kok DJ (2000) Role of macrophages in nephrolithiasis in rats: an analysis of the renal interstitium. Am J Kidney Dis 36:615–625
27. de Water R, Leenen PJ, Noordermeer C, Nigg AL, Houtsmuller AB, Kok DJ, Schröder FH (2001) Cytokine production induced by binding and processing of calcium oxalate crystals. Am J Kidney Dis 38:331–338
28. Mandel NS, Mandel GS (1989) Urinary tract stone incidence in the US veteran population: II. Geographical analysis of variations in composition. J Urol 142:1516–1521
29. Dyer R, Nordin BE (1967) Urinary crystals and their relation to stone formation. Nature 215:751–752
30. Elliot JS, Rabinowitz IN (1980) Calcium oxalate crystalluria: crystal size in urine. J Urol 123:324–327
31. Wesson JA, Worcester E (1996) Formation of hydrated calcium oxalates in the presence of poly-L-aspartic acid. Scanning Microsc Int 10:415–424
32. Wesson JA, Worcester EM, Wiessner JH, Mandel NS, Kleinmann JG (1998) Control of calcium oxalate crystal structure and cell adherence by urinary macromolecules. Kidney Int 53:952–957
33. Lieske JC, Leonard R, Toback FG (1995) Adhesion of calcium oxalate monohydrate crystals to renal epithelial cells is inhibited by specific anions. Am J Physiol 268:F604–F612
34. Kumar V, Farell G, Lieske JC (2003) Whole urinary proteins coat calcium oxalate monohydrate crystals to greatly decrease their adhesion to renal cells. J Urol 170:221–225
35. Grover PK, Thurgood LA, Ryall RL (2007) Effect of urine fractionation on attachment of calcium oxalate crystals to renal epithelial cells: implications for studying renal calculogenesis. Am J Physiol Renal Physiol 292:F1396–F1403
36. Grover PK, Wang T, Thurgood LA, Ryall RL (2009) The effects of intracrystalline and surface-bound proteins on the attachment of calcium oxalate monohydrate crystals to renal cells in undiluted human urine. BJU Int (epub)
37. Chien YC, Masica DL, Gray JJ, Nguyen S, Vali H, McKee MD (2009) Modulation of calcium oxalate dihydrate crystal growth by selective crystal face binding of phosphorylated osteopontin and poly-aspartate peptide showing occlusion by sectoral (compositional) zoning. J Biol Chem 284:23491–23501
38. Qiu SR, Wierzbicki A, Orme CA, Cody AM, Hoyer JR, Nancollas GH, Zepeda S, De Yoreo JJ (2004) Molecular modulation of calcium oxalate crystallization by osteopontin and citrate. Proc Natl Acad Sci 101:1811–1815
39. Taller A, Grohe B, Rogers KA, Goldberg HA, Hunter GK (2007) Specific adsorption of osteopontin and synthetic polypeptides to calcium oxalate monohydrate crystals. Biophys J 93:1768–1777
40. Grohe B, O'Young J, Ionescu DA, Lajoie G, Rogers KA, Karttunen M, Goldberg HA, Hunter GK (2007) Control of calcium oxalate crystal growth by face-specific adsorption of an osteopontin phosphopeptide. J Am Chem Soc 129:14946–14951
41. O'Young J, Chirico S, Al Tarhuni N, Grohe B, Karttunen M, Goldberg HA, Hunter GK (2009) Phosphorylation of osteopontin peptides mediates adsorption to and incorporation into calcium oxalate crystals. Cells Tissues Organs 189:51–55
42. Senger DR, Perruzzi CA, Papadopoulos A, Tenen DG (1989) Purification of a human milk protein closely similar to tumor-secreted phosphoproteins and osteopontin. Biochim Biophys Acta 996:43–48
43. Ryall RL, Grover PK, Thurgood LA, Chauvet MC, Fleming DE, van Bronswijk W (2007) The importance of a clean face: the effect of different washing procedures on the association of Tamm-Horsfall glycoprotein and other urinary proteins with calcium oxalate crystals. Urol Res 35:1–14
44. Bautista DS, Denstedt J, Chambers AF, Harris JF (1996) Low-molecular-weight variants of osteopontin generated by serine proteinases in urine of patients with kidney stones. J Cell Biochem 61:402–409
45. Hoyer JR, Pietrzyk RA, Liu H, Whitson PA (1999) Effects of microgravity on urinary osteopontin. J Am Soc Nephrol 10:S389–S393
46. Thurgood LA, Grover PK, Ryall RL (2008) High calcium concentration and calcium oxalate crystals cause significant inaccuracies in the measurement of urinary osteopontin by enzyme linked immunosorbent assay. Urol Res 36:103–110
47. Min W, Shiraga H, Chalko C, Goldfarb S, Krishna GG, Hoyer JR (1998) Quantitative studies of human urinary excretion of uropontin. Kidney Int 53:189–193
48. Cook AF, Grover PK, Ryall RL (2008) Face-specific binding of prothrombin fragment 1 and human serum albumin to inorganic and urinary calcium oxalate monohydrate crystals. BJU Int 103:826–835

49. Hess B, Ryall RL, Kavanagh JP, Khan SR, Kok D-J, Rodgers AL, Tiselius H-G (2001) Methods for measuring crystallization in urolithiasis research—why, how and when? Eur Urol 40:220–230
50. Brown LF, Berse B, Van de Water L, Papadopoulos-Sergiou A, Perruzzi CA, Manseau EJ, Dvorak HF, Senger DR (1992) Expression and distribution of osteopontin in human tissues: widespread association with luminal epithelial surfaces. Mol Biol Cell 3:1169–1180
51. Jung T, Sheng X, Choi CK, Kim WS, Wesson JA, Ward MD (2004) Probing crystallization of calcium oxalate monohydrate and the role of macromolecule additives with in situ atomic force microscopy. Langmuir 20:8587–8596
52. Millan A (2001) Crystal growth shape of whewellite polymorphs: influence of structure distortions on crystal shape. Cryst Growth Des 1:245–254
53. Ryall RL, Fleming DE, Doyle IR, Evans NA, Dean CJ, Marshall VR (2001) Intracrystalline proteins and the hidden ultrastructure of calcium oxalate urinary crystals: implications for kidney stone formation. J Struct Biol 134:5–14
54. Ryall RL, Fleming DE, Grover PK, Chauvet MC, Dean CJ, Marshall VR (2000) The hole truth: intracrystalline proteins and calcium oxalate kidney stones. Mol Urol 4:391–402
55. Ryall RL (2004) Macromolecules and urolithiasis: parallels and paradoxes. Nephron 98:37–42
56. Khan SR, Kok DJ (2004) Modulation of urinary stone formation. Front Biosci 9:1450–1482
57. Chauvet MC, Ryall RL (2005) Intracrystalline proteins and calcium oxalate crystal degradation in MDCK II cells. J Struct Biol 151:12–17
58. Grover PK, Thurgood LA, Fleming DE, van Bronswijk W, Wang T, Ryall RL (2008) Intracrystalline urinary proteins facilitate degradation and dissolution of calcium oxalate crystals in cultured renal cells. Am J Physiol 294:F336–F355
59. Wang L, Guan X, Tang R, Hoyer JR, Wierzbicki A, De Yoreo JJ, Nancollas GH (2008) Phosphorylation of osteopontin in required for inhibition of calcium oxalate crystallization. J Phys Chem B 112:9151–9157
60. Christensen B, Petersen TE, Sørensen ES (2008) Post-translational modification and proteolytic processing of urinary osteopontin. Biochem J 411:53–61
61. Kon S, Maeda M, Segawa T, Hagiwara Y, Horikoshi Y, Chikuma S, Tanaka K, Rashid MM, Inobe M, Chambers AF, Uede T (2000) Antibodies to different peptides in osteopontin reveal complexities in the various secreted forms. J Cell Biochem 77:487–498
62. Hunter GK, Kyle CL, Goldberg HA (1994) Modulation of crystal formation by bone phosphoproteins: structural specificity of the osteopontin-mediated inhibition of hydroxyapatite formation. Biochem J 300:723–728
63. Giachelli CM, Steitz S (2000) Osteopontin: a versatile regulator of inflammation and biomineralization. Matrix Biol 19:612–622
64. Kasemo B, Lausmaa J (1994) Material-tissue interfaces: the role of surface properties and processes. Environ Health Perspect 102(Suppl 5):41–45
65. Boskey AL (1995) Osteopontin and related phosphorylated sialoproteins: effects on mineralization. Ann N Y Acad Sci 760:249–256
66. Beshensky AM, Wesson JA, Worcester EM, Sorokina EJ, Snyder CJ, Kleinman JG (2001) Effects of urinary macromolecules on hydroxyapatite crystal formation. J Am Soc Nephrol 12:2108–2116
67. Guo SW, Ward MD, Wesson JA (2002) Direct visualization of calcium oxalate monohydrate crystallization and dissolution with atomic force microscopy and the role of polymeric additives. Langmuir 18:4284–4291
68. Grohe B, Taller A, Vincent PL, Tieu LD, Rogers KA, Heiss A, Sørensen ES, Mittler S, Goldberg H, Hunter GK (2009) Crystallization of calcium oxalate is controlled by molecular hydrophilicity and specific polyanion-crystal interactions. Langmuir 25:11635–11646
69. Asplin JR, Arsenault D, Parks JH, Coe FL, Hoyer JR (1998) Contribution of human uropontin to inhibition of calcium oxalate crystallization. Kidney Int 53:194–199
70. Sheng X, Ward MD, Wesson JA (2005) Crystal surface adhesion explains the pathological activity of calcium oxalate hydrates in kidney stone formation. J Am Soc Nephrol 16:1904–1908
71. Chen Y, Bal BS, Gorski JP (1992) Calcium and collagen binding properties of osteopontin, bone sialoprotein, and bone acidic glycoprotein-75 from bone. J Biol Chem 267:24871–24878
72. Tazzoli V, Domeneghetti C (1980) The crystal structures of whewellite and weddellite: re-examination and comparison. Am Mineral 65:327–334